

Fast Algorithms and Theory for High-Dimensional Bayesian Varying Coefficient Models *

Ray Bai^{††}; Mary R. Boland[†]; Yong Chen[†]

December 21, 2024

Abstract

Nonparametric varying coefficient (NVC) models are widely used for modeling time-varying effects on responses that are measured repeatedly. In this paper, we introduce the *nonparametric varying coefficient spike-and-slab lasso* (NVC-SSL) for Bayesian estimation and variable selection in NVC models. The NVC-SSL simultaneously estimates the functionals of the significant time-varying covariates while thresholding out insignificant ones. Our model can be implemented using a highly efficient expectation-maximization (EM) algorithm, thus avoiding the computational intensiveness of Markov chain Monte Carlo (MCMC) in high dimensions. In contrast to frequentist NVC models, hardly anything is known about the large-sample properties for Bayesian NVC models. In this paper, we take a step towards addressing this long-standing gap between methodology and theory by deriving posterior contraction rates under the NVC-SSL model when the number of covariates grows at nearly exponential rate with sample size. Finally, we illustrate our methodology through simulation studies and data analysis.

*Keywords and phrases: spike-and-slab, spike-and-slab group lasso, posterior contraction, variable selection, varying coefficient model

[†]Department of Biostatistics, Epidemiology, and Informatics, University of Pennsylvania, Philadelphia, PA 19104.

^{††}Email: Ray.Bai@pennmedicine.upenn.edu

1 Introduction

Consider the nonparametric varying coefficient (NVC) model with p covariates,

$$y_i(t_{ij}) = \sum_{k=1}^p x_{ik}(t_{ij})\beta_k(t_{ij}) + \varepsilon_i(t_{ij}), \quad i = 1, \dots, n, \quad j = 1, \dots, n_i, \quad (1.1)$$

where $y_i(t)$ is the response for the i th subject at time point $t \in T$, T is the time interval on which the n_i different measurements are taken, $x_{ik}(t)$ is a time-dependent covariate with corresponding smooth coefficient function $\beta_k(t)$, and $\varepsilon_i(t)$ is random error. Throughout this paper, we denote $N = \sum_{i=1}^n n_i$ as the total number of observations. To avoid the need for an intercept, we assume the within-subject responses have been centered, i.e. $\sum_{j=1}^{n_i} y_i(t_{ij}) = 0, i = 1, \dots, n$. We also assume that the $\varepsilon_i(t)$'s are independent, zero-mean Gaussian processes. That is, we assume that $\varepsilon_i = (\varepsilon_1(t_{i1}), \dots, \varepsilon_i(t_{in_i}))' \sim \mathcal{N}_{n_i}(\mathbf{0}, \Sigma_i), i = 1, \dots, n$, where Σ_i is the variance-covariance matrix that captures the temporal correlation between the n_i responses, y_{i1}, \dots, y_{in_i} , for the i th subject.

NVC models (1.1) arise in many real applications. A prominent example is in longitudinal data analysis where we aim to model the response for the i th experimental subject at n_i different time points [14]. NVC models can also be used for functional data analysis where we wish to model smooth functional responses $y_i(t), i = 1, \dots, n$, varying over a continuum $t \in T$ [29]. See [12, 9] for examples of applications of these models. We note that while we model the response as a function of time $y(t)$ in this manuscript, the model (1.1) can also be used more broadly to model functions $y(z)$ of any “effect modifier” variable z , such as spatial location, wavelength, etc. [12].

There has been extensive frequentist work on fitting NVC models. Typical approaches to fitting (1.1) use kernel-local polynomial smoothing [8, 36] or basis expansions [16, 28] to estimate $\beta_k(t), k = 1, \dots, p$. When the number of covariates p is large, one also often wants to impose a low-dimensional structure such as sparsity. In order to perform simultaneous function estimation and model selection, many authors have applied a penalty such as group SCAD [7] or group lasso [38] to the vectors of basis coefficients. See, e.g. [33, 34, 35]. These frequentist penalized NVC models do not account for the within-subject temporal correlations, essentially solving objective functions with $\varepsilon = (\varepsilon_1', \dots, \varepsilon_n')' \sim \mathcal{N}_N(\mathbf{0}, \mathbf{I}_N)$. In low-dimensional settings and without regularizing the parameter space, Krafty et al. [20] incorporated estimation of within-subject correlations into NVC models. However,

to the best of our knowledge, no similar extension has been made for high-dimensional, penalized NVC models. While [33, 34, 35] show that consistent estimation of the β_k 's and model selection consistency can still be achieved for penalized NVC models, failing to account for the error variances can nevertheless lead to invalid inferences and overfitting in finite samples [24, 26]. Thus, it seems prudent to model temporal dependence in NVC models.

While there are numerous theoretical results for frequentist NVC models, work on Bayesian NVC models has been primarily methodological. For example, Liu et al. [25] endow the smooth functions $\beta_k(t)$'s with a Gaussian process prior. Biller and Fahrmeir [3] and Huang et al. [17] use splines to model the $\beta_k(t)$'s in (1.1) and place multivariate normal priors on the groups of basis coefficients. Li et al. [22] place a scale-mixture of a multivariate normal priors known as the Bayesian group lasso prior on groups of basis coefficients. Unlike the frequentist penalized approaches, [25, 22] explicitly model the temporal dependence of the within-subject measurements by either including subject-specific random effects or by specifying a first-order autoregressive (AR(1)) covariance structure for the error terms $\varepsilon_i(t)$. In spite of the benefits of being able to incorporate covariance structure into variable selection, existing Bayesian approaches to NVCs predominantly rely on Markov chain Monte Carlo (MCMC) to obtain posterior estimates of the $\beta_k(t)$'s. In high dimensions, however, MCMC can be very slow and even computationally impractical. In addition, hardly anything is known about the theoretical properties for Bayesian NVC models.

In this paper, we take a step towards addressing these methodological, computational, and theoretical gaps by introducing the *nonparametric varying coefficient spike-and-slab lasso* (NVC-SSL). Our main contributions are as follows:

- We introduce a spike-and-slab approach for Bayesian estimation and variable selection in nonparametric varying coefficient models (1.1). Unlike penalized frequentist approaches, the NVC-SSL model explicitly accounts for temporal correlations by *jointly* estimating the unknown covariance structure for the time-varying responses. The NVC-SSL model also employs a *non*-separable Bayesian penalty which automatically self-adapts to ensemble information about sparsity.
- We derive an expectation/maximization (EM) algorithm to rapidly select and estimate the nonzero smooth functional components, while thresholding out the insignificant ones. Our paper appears to be the first to bypass MCMC in its implementation of a Bayesian NVC model.

- We provide the first theoretical results for Bayesian varying coefficient models when $p \gg n$. Specifically, we derive posterior contraction rates for the functional components when the number of time-dependent covariates p grows at nearly exponential rate with n .

The rest of this paper is structured as follows. In Section 2, we introduce the nonparametric varying coefficient spike-and-slab lasso. In Section 3, we derive a coordinate ascent algorithm for rapidly obtaining estimates of the smooth functionals $\beta_k(t)$, $k = 1, \dots, p$, under the NVC-SSL. In Section 4, we provide asymptotic theory for the NVC model (1.1) under the NVC-SSL prior when $p \gg n$. In Section 5, we provide simulation studies of our method. Finally, in Section 6, we use our model to analyze a real data set.

1.1 Notation

We use the following notations for the rest of the paper. For two nonnegative sequences $\{a_n\}$ and $\{b_n\}$, we write $a_n \asymp b_n$ to denote $0 < \liminf_{n \rightarrow \infty} a_n/b_n \leq \limsup_{n \rightarrow \infty} a_n/b_n < \infty$. If $\lim_{n \rightarrow \infty} a_n/b_n = 0$, we write $a_n = o(b_n)$ or $a_n \prec b_n$. We use $a_n \lesssim b_n$ or $a_n = O(b_n)$ to denote that for sufficiently large n , there exists a constant $C > 0$ independent of n such that $a_n \leq Cb_n$. We write $a_n \vee b_n$ to denote $\max\{a_n, b_n\}$.

For a vector $\mathbf{v} \in \mathbb{R}^p$, we let $\|\mathbf{v}\|_2 := \sqrt{\sum_{i=1}^p v_i^2}$ and $\|\mathbf{v}\|_\infty := \max_i |v_i|$ denote the ℓ_2 and ℓ_∞ norms respectively. For a symmetric matrix \mathbf{A} , we let $\lambda_{\min}(\mathbf{A})$ and $\lambda_{\max}(\mathbf{A})$ denote its minimum and maximum eigenvalues respectively. For a matrix $\mathbf{A} \in \mathbb{R}^{a \times b}$ with entries a_{ij} , $\|\mathbf{A}\|_F := \sqrt{\text{tr}(\mathbf{A}'\mathbf{A})} = \sqrt{\sum_{i=1}^a \sum_{j=1}^b a_{ij}^2}$ denotes its Frobenius norm, while $\|\mathbf{A}\|_2 := \sqrt{\lambda_{\max}(\mathbf{A}'\mathbf{A})}$ denotes its spectral norm.

2 The Nonparametric Varying Coefficient Spike-and-Slab Lasso

2.1 Basis Expansion and the NVC-SSL

Following the development in [33, 34, 35], we suppose that each coefficient function β_k in (1.1) can be approximated by g_k , a linear combination of d_k basis functions, i.e.

$$g_k(t) = \sum_{l=1}^{d_k} \gamma_{kl} B_{kl}(t), t \in T, k = 1, \dots, p, \quad (2.1)$$

where $B_{kl}(t), t \in T, l = 1, \dots, d_k$, are the basis functions. Then the model (1.1) can be approximated as

$$y_i(t_{ij}) \approx \sum_{k=1}^p \sum_{l=1}^{d_k} x_{ik}(t_{ij}) \gamma_{kl} B_{kl}(t_{ij}) + \varepsilon_i(t_{ij}), \quad (2.2)$$

for $i = 1, \dots, n$ and $j = 1, \dots, n_i$. Let $\mathbf{X} = [\mathbf{X}_1, \dots, \mathbf{X}_p]$, with

$$\mathbf{X}_k = (x_{1k}(t_{11}), \dots, x_{1k}(t_{1n_1}), \dots, x_{nk}(t_{n1}), \dots, x_{nk}(t_{nn_n}))'. \quad (2.3)$$

Further, we define $\mathbf{B}(t)$ as

$$\mathbf{B}(t) = \begin{pmatrix} B_{11}(t) & B_{12}(t) & \dots & B_{1d_1}(t) & 0 & \dots & 0 & 0 & \dots & 0 \\ \vdots & \vdots & & \vdots & \vdots & & \vdots & \vdots & & \vdots \\ 0 & 0 & \dots & 0 & 0 & \dots & B_{p1}(t) & B_{p2}(t) & \dots & B_{pd_p}(t) \end{pmatrix}, \quad (2.4)$$

and set $\mathbf{U} = (\mathbf{U}_{11}, \dots, \mathbf{U}_{1n_1}, \dots, \mathbf{U}_{n1}, \dots, \mathbf{U}_{nn_n})'$ with

$$\mathbf{U}'_{ij} = \mathbf{x}'(t_{ij}) \mathbf{B}(t_{ij}) \quad (2.5)$$

for $i = 1, \dots, n, j = 1, \dots, n_i$, where $\mathbf{x}'(t_{ij})$ denotes the row of \mathbf{X} corresponding to the j th observation for the i th subject.

Letting $\mathbf{Y} = (y_1(t_{11}), \dots, y_1(t_{1n_1}), \dots, y_n(t_{n1}), \dots, y_n(t_{nn_n}))'$ and $\varepsilon = (\varepsilon'_1, \dots, \varepsilon'_n)'$, the model (1.1) can then be expressed in matrix form as

$$\mathbf{Y} - \boldsymbol{\delta} = \mathbf{U} \boldsymbol{\gamma} + \varepsilon, \quad \varepsilon \sim \mathcal{N}_N(\mathbf{0}, \boldsymbol{\Sigma}), \quad (2.6)$$

where $\boldsymbol{\gamma} = (\boldsymbol{\gamma}'_1, \dots, \boldsymbol{\gamma}'_p)'$ and $\boldsymbol{\gamma}_k = (\gamma_{k1}, \dots, \gamma_{kd_k})'$, $k = 1, \dots, p$, is the d_k -dimensional vector of basis coefficients corresponding to the k th covariate. $\boldsymbol{\Sigma} = \text{diag}(\boldsymbol{\Sigma}_1, \dots, \boldsymbol{\Sigma}_n)$ is an $N \times N$ block diagonal matrix, and $\boldsymbol{\delta}$ is an $N \times 1$ vector of lower-order bias, or the approximation error from using truncated bases of dimension d_k to approximate the β_k 's.

2.2 Model Formulation

For the NVC model (1.1), we assume that the within-subject covariance matrices have the structure, $\boldsymbol{\Sigma}_i = \sigma^2 \mathbf{R}_i(\rho)$, $i = 1, \dots, n$, where $\mathbf{R}_i(\rho)$ denotes that the correlation matrix \mathbf{R}_i is determined by a single parameter $\rho \in (0, 1)$. That is, we suppose that for $\varepsilon = (\varepsilon'_1, \dots, \varepsilon'_n)'$,

$$\varepsilon_i \stackrel{ind}{\sim} \mathcal{N}_{n_i} \left(\mathbf{0}, \sigma^2 \mathbf{R}_i(\rho) \right), i = 1, \dots, n. \quad (2.7)$$

This general form subsumes many popular choices for covariance structures. For example, if we assume first-order autoregressive (AR(1)) structure, then the (j, k) th element of $\mathbf{R}_i(\rho)$ is $\rho^{|t_{ij} - t_{ik}|}$. For compound symmetry (CS), the (j, k) th element of $\mathbf{R}_i(\rho)$ is $\mathbb{I}(j = k) + \rho\mathbb{I}(j \neq k)$. For concreteness, we focus only on AR(1) and CS structures in this paper, noting that our model can be generalized to more exotic correlation structures. This assumption about the structure of the Σ_i 's makes our estimation procedure more computationally efficient and less prone to overfitting, as the problem of estimating $N + \sum_{i=1}^n n_i(n_i - 1)/2$ unknowns (the number of diagonal and unique off-diagonal entries in the Σ_i 's) reduces to just estimating two unknowns (σ^2, ρ).

Under the NVC-SSL model, we endow the vector of basis coefficients $\gamma = (\gamma'_1, \dots, \gamma'_p)'$ in (2.6) with the *spike-and-slab group lasso* (SSGL) prior of [2],

$$\pi(\gamma|\theta) = \prod_{k=1}^p [(1 - \theta)\Psi(\gamma_k|\lambda_0) + \theta\Psi(\gamma_k|\lambda_1)], \quad (2.8)$$

where θ is a mixing proportion, or the expected proportion of nonzero γ_k 's, and $\Psi(\cdot|\lambda)$ denotes the group lasso density indexed by hyperparameter λ ,

$$\Psi(\gamma_k|\lambda) = \frac{\lambda^{d_k} e^{-\lambda\|\gamma_k\|_2}}{2^{d_k} \pi^{(d_k-1)/2} \Gamma((d_k + 1)/2)}, \quad k = 1, \dots, p.$$

The group lasso prior has been considered by several other authors [2, 22, 21, 37] and can be derived as the marginal density of a multivariate normal scale-mixture density, $\gamma_k|\zeta \sim \mathcal{N}_{d_k}(\mathbf{0}_{d_k}, \zeta \mathbf{I}_{d_k})$, $\zeta \sim \mathcal{G}((d_k + 1)/2, \lambda^2/2)$.

The SSGL prior (2.8), which we denote as $\mathcal{SSGL}(\lambda_0, \lambda_1, \theta)$ going forward, can be considered a two-group refinement of the group lasso [38]. Under the prior (2.8), the global posterior mode for γ may be exactly sparse, thereby allowing the $\mathcal{SSGL}(\lambda_0, \lambda_1, \theta)$ to perform joint estimation and variable selection [2]. In the present context, if the posterior mode $\hat{\gamma}_k = \mathbf{0}_{d_k}$, then the k th functional component will be estimated as $\hat{\beta}_k(t) = \sum_{l=1}^{d_k} \hat{\gamma}_{kl} B_{kl}(t) = 0$ and thus thresholded out of the model. We typically set $\lambda_0 \gg \lambda_1$ in (2.8), so that the first mixture component (the spike) is heavily concentrated near $\mathbf{0}_{d_k}$ for each $k = 1, \dots, p$, while the slab stabilizes the posterior estimates of large coefficients, preventing them from being downward biased.

To model the uncertainty in θ in (2.8), we endow θ with a beta prior,

$$\theta \sim \mathcal{B}(a, b), \quad (2.9)$$

where (a, b) are fixed positive constants. Unlike frequentist penalties such as group SCAD or group lasso, this prior on θ ultimately renders our Bayesian

penalty *non*-separable. The non-separability provides several benefits. First, the prior on θ allows $\mathcal{SSGL}(\lambda_0, \lambda_1, \theta)$ to self-adapt to the true underlying sparsity. Second, with appropriate choices for the hyperparameters in $\theta \sim \mathcal{B}(a, b)$, namely $a = 1, b = p$, our prior performs an automatic multiplicity adjustment [32] and favors parsimonious models in high dimensions.

To complete the model specification, we place independent priors on the parameters (σ^2, ρ) in (2.7) as

$$\sigma^2 \sim \mathcal{IG}(c_0/2, d_0/2), \quad (2.10)$$

where $c_0, d_0 > 0$ are small positive constants, and

$$\pi(\rho) = \sum_{h=1}^q q^{-1} \delta_{m_h}. \quad (2.11)$$

That is, ρ follows a discrete uniform distribution with q atoms $\{m_1, \dots, m_q\}$ where $0 < m_h < 1, 1 \leq h \leq q$. In our implementation, we specify the support for $\pi(\rho)$ as $\{0.05, 0.10, \dots, 0.95\}$. As we describe in Section 3, placing a discrete uniform prior on ρ facilitates more efficient computations (from an optimization perspective) than a continuous prior with bounded support.

2.3 Determining Which Covariance Structure to Use

Our model requires the user to specify the error covariance structure (AR(1) or CS). In order to determine which one to use, we can first obtain the residuals $\hat{y}(t_{ij}) - y(t_{ij})$ from a regression fit (e.g. a regression with the standard group lasso). Then we can construct empirical variogram plots, time-plots, or scatterplot matrices of the residuals to give us an idea of the underlying error covariance structure [5].

In particular, the empirical variogram of the residuals (see Chapter 5 of [5]) is widely used in practice to determine the appropriate covariance structure to use for modeling longitudinal and spatial data. If the residual variogram shows decaying correlation with distance, then we may specify the AR(1) structure for the NVC-SSL model. On the other hand, if the residual variogram suggests equicorrelation, then we may specify the CS structure.

3 Computational Strategy

3.1 Posterior Mode Estimation

We now detail how to implement the NVC-SSL model. Rather than relying on MCMC, we will target the maximum *a posteriori* (MAP) estimate for

the basis coefficients, $\hat{\gamma}$. We may then take as our estimates for the smooth functionals as $\hat{\beta}_k(t) = \sum_{l=1}^d \hat{\gamma}_{kl} B_{kl}(t)$, $k = 1, \dots, p$. For simplicity, we let the basis truncation parameters satisfy $d_1 = \dots d_p = d$ for some positive integer d . In Section 3.3, we describe how to select d .

Let Ξ denote the collection $\{\gamma, \theta, \sigma^2, \rho\}$. The log-posterior density for Ξ (up to an additive constant) is given by

$$\begin{aligned} \log \pi(\Xi | \mathbf{Y}) = & -\frac{N}{2} \log \sigma^2 - \frac{1}{2} \log |\mathbf{R}(\rho)| - \frac{\|\mathbf{R}^{-1/2}(\rho)(\mathbf{Y} - \mathbf{U}\gamma)\|_2^2}{2\sigma^2} \\ & + \sum_{k=1}^p \log \left((1-\theta)\lambda_0^d e^{-\lambda_0 \|\gamma_k\|_2} + \theta\lambda_1^d e^{-\lambda_1 \|\gamma_k\|_2} \right) \\ & + (a-1) \log \theta + (b-1) \log(1-\theta) \\ & - \left(\frac{c_0+2}{2} \right) \log \sigma^2 - \frac{d_0}{2\sigma^2} + \log \pi(\rho). \end{aligned} \quad (3.1)$$

Our objective is to maximize the log-posterior with respect to Ξ . We first introduce latent 0-1 indicators, $\boldsymbol{\tau} = (\tau_1, \dots, \tau_p)'$. Then we reparametrize the $\mathcal{SSGL}(\lambda_0, \lambda_1, \theta)$ prior (2.8) as:

$$\begin{aligned} \pi(\gamma | \boldsymbol{\tau}) &= \prod_{k=1}^p [(1-\tau_k)\boldsymbol{\Psi}(\gamma_k | \lambda_0) + \tau_k \boldsymbol{\Psi}(\gamma_k | \lambda_1)], \\ \pi(\boldsymbol{\tau} | \theta) &= \prod_{k=1}^p \theta^{\tau_k} (1-\theta)^{1-\tau_k}. \end{aligned}$$

Let $\mathbf{R} := \mathbf{R}(\rho) = \text{diag}(\mathbf{R}_1(\rho), \dots, \mathbf{R}_n(\rho))$. The augmented log-posterior density for $(\Xi, \boldsymbol{\tau})$ (up to an additive constant) is now given by

$$\begin{aligned} \log \pi(\Xi, \boldsymbol{\tau} | \mathbf{Y}) = & -\frac{N}{2} \log \sigma^2 - \frac{1}{2} \log |\mathbf{R}(\rho)| - \frac{\|\mathbf{R}^{-1/2}(\rho)(\mathbf{Y} - \mathbf{U}\gamma)\|_2^2}{2\sigma^2} \\ & + \sum_{k=1}^p \log \left((1-\tau_k)\lambda_0^d e^{-\lambda_0 \|\gamma_k\|_2} + \tau_k \lambda_1^d e^{-\lambda_1 \|\gamma_k\|_2} \right) \\ & + \left(a-1 + \sum_{k=1}^p \tau_k \right) \log \theta + \left(b-1 + p - \sum_{k=1}^p \tau_k \right) \log(1-\theta) \\ & - \left(\frac{c_0+2}{2} \right) \log \sigma^2 - \frac{d_0}{2\sigma^2} + \log \pi(\rho). \end{aligned} \quad (3.2)$$

It is straightforward to verify that $\mathbb{E}[\tau_k | \mathbf{Y}, \Xi] = p_k^*(\gamma_k, \theta)$, where

$$p_k^*(\gamma_k, \theta) = \frac{\theta \boldsymbol{\Psi}(\gamma_k | \lambda_1)}{\theta \boldsymbol{\Psi}(\gamma_k | \lambda_1) + (1-\theta) \boldsymbol{\Psi}(\gamma_k | \lambda_0)} \quad (3.3)$$

is the conditional posterior probability that γ_k is drawn from the slab distribution rather than from the spike.

With the augmented log-posterior (3.2), we may now implement an EM algorithm to find Ξ^* . After initializing the parameters $\Xi^{(0)}$, we iterate between the E-step and M-step until convergence. For the E-step, we compute $p_k^* := p^*(\gamma_k^{(t-1)}, \theta^{(t-1)}) = \mathbb{E}[\tau_k | \mathbf{Y}, \Xi^{(t-1)}]$, given the previous estimate $\Xi^{(t-1)}$. For the M-step, we then maximize the following objective function with respect to Ξ :

$$\begin{aligned} & \mathbb{E} \left[\log(\Xi | \mathbf{Y}) | \Xi^{(t-1)} \right] \\ &= -\frac{N}{2} \log \sigma^2 - \frac{1}{2} \log |\mathbf{R}(\rho)| - \frac{\|\mathbf{R}^{-1/2}(\rho)(\mathbf{Y} - \mathbf{U}\gamma)\|_2^2}{2\sigma^2} - \sum_{k=1}^p \lambda_k^* \|\gamma_k\|_2 \\ &+ \left(a - 1 + \sum_{k=1}^p p_k^* \right) \log \theta + \left(b - 1 + p - \sum_{k=1}^p p_k^* \right) \log(1 - \theta) \\ & - \left(\frac{c_0 + 2}{2} \right) \log \sigma^2 - \frac{d_0}{2\sigma^2} + \log \pi(\rho), \end{aligned} \quad (3.4)$$

where $\lambda_k^* = \lambda_1 p_k^* + \lambda_0 (1 - p_k^*)$. The function (3.4) would be difficult to jointly maximize with respect to $(\gamma, \rho, \theta, \sigma^2)$ if $\pi(\rho)$ were a continuous density. However, by endowing ρ with a discrete uniform prior (2.11), our optimization is much simpler. With the prior (2.11), we may fix $\rho \in \{m_1, \dots, m_q\}$ and maximize (3.4) with respect to $(\gamma, \theta, \sigma^2)$ for each atom. In our implementation, each of these t optimizations is performed in parallel and the log-posterior for each m_h , $1 \leq h \leq q$, is evaluated. We take as our modal estimate the $\hat{\rho}$ to be the m_h which maximizes $\log \pi(\hat{\gamma}, \hat{\theta}, \hat{\sigma}^2, \rho | \mathbf{Y}, \rho = m_h)$, the original non-augmented log-posterior (3.1).

For either fixed or random ρ , it is clear from (3.4) that θ has the following closed form update in the M-step:

$$\theta^{(t)} = \frac{a - 1 + \sum_{k=1}^p p_k^*}{a + b + p - 2}. \quad (3.5)$$

Next, we update γ , holding $(\theta, \sigma^2, \rho) = (\theta^{(t)}, \sigma^{2(t-1)}, m_h)$ fixed. Let $\widetilde{\mathbf{Y}} = \mathbf{R}^{-1/2}(m_h)\mathbf{Y}$ and $\widetilde{\mathbf{U}} = \mathbf{R}^{-1/2}(m_h)\mathbf{U}$. To update γ , we solve the following optimization:

$$\gamma^{(t)} = \arg \max_{\gamma} -\frac{1}{2} \|\widetilde{\mathbf{Y}} - \widetilde{\mathbf{U}}\gamma\|_2^2 - \sum_{k=1}^p \sigma^2 \lambda_k^* \|\gamma_k\|_2. \quad (3.6)$$

Note that (3.6) is an adaptive group lasso problem with weights $\sigma^2 \lambda_k^*$, and it explicitly takes temporal correlation into account (through \mathbf{R}) in our

estimate procedure for γ . This optimization can be solved with any standard (adaptive) group lasso algorithm [38, 13].

Finally, holding $(\gamma, \rho) = (\gamma^{(t)}, m_h)$ fixed, we update σ^2 , which has the following closed form:

$$\sigma^{2(t)} = \frac{d_0 + \|\widetilde{\mathbf{Y}} - \widetilde{\mathbf{U}}\gamma\|_2^2}{N + c_0 + 2}. \quad (3.7)$$

In order to obtain $\widetilde{\mathbf{Y}}$ and $\widetilde{\mathbf{U}}$ and evaluate the log posterior (3.1) for each atom $m_h, 1 \leq h \leq q$, in (2.11), we must invert \mathbf{R} , which is an $N \times N$ matrix. However, by exploiting the block structure of \mathbf{R} , we only need to perform n matrix inversions of the individual correlation matrices $\mathbf{R}_i, i = 1, \dots, n$, incurring total computational complexity of $\sum_{i=1}^n \mathcal{O}(n_i^3)$. Similarly, evaluating the log-determinant $\log|\mathbf{R}| = \sum_{k=1}^n \log|\mathbf{R}_i|$ requires $\sum_{i=1}^n \mathcal{O}(n_i^3)$ operations. In high dimensions, n_i is typically smaller than both n and p , so performing these operations is not particularly costly. To further improve computational efficiency, we compute the inverses and log-determinants of the \mathbf{R}_i 's in parallel. Letting \mathbf{Y}_i and \mathbf{U}^i denote the subvector and submatrix of \mathbf{Y} and \mathbf{U} corresponding to the i th subject respectively, we also compute $\widetilde{\mathbf{Y}}_i = \mathbf{R}_i^{-1/2} \mathbf{Y}_i, i = 1, \dots, n$, and $\widetilde{\mathbf{U}}^i = \mathbf{R}_i^{-1/2} \mathbf{U}^i, i = 1, \dots, n$, in parallel and then combine them into a single $\widetilde{\mathbf{Y}}$ and $\widetilde{\mathbf{U}}$ respectively.

3.2 Initialization and Dynamic Posterior Exploration

The posterior distribution under the NVC-SSL prior will typically be multimodal when $p \gg n$ and $\lambda_0 \gg \lambda_1$, and thus, any MAP finding algorithm is prone to becoming entrapped at a suboptimal local mode. To partially mitigate this, we initialize our EM algorithm at $\gamma^{(0)}$, where $\gamma^{(0)}$ is the group lasso solution without accounting for any temporal correlations. That is,

$$\gamma^{(0)} = \arg \max_{\gamma} \frac{1}{2} \|\mathbf{Y} - \mathbf{U}\gamma\|_2^2 + \lambda \sum_{k=1}^p \sqrt{d} \|\gamma_k\|_2,$$

where $\lambda > 0$ is chosen from ten-fold cross-validation. The initial unknown variance $\sigma^{2(0)}$ is also taken to be $\sigma^{2(0)} = \|\mathbf{Y} - \mathbf{U}\gamma^{(0)}\|_2^2/N$. In our experience, this initialization works well in ensuring rapid convergence to a fairly good solution, even though we are not guaranteed to find the global mode. Even if we were to implement our model using MCMC, the model with the highest posterior probability may only be visited a small number of times or may never even be visited at all (see, e.g. Section 4.3 of [30]).

In addition to choosing a good initialization, we employ *dynamic posterior exploration* to increase the chances of finding more optimal modes [31, 30, 2]. We fix λ_1 to be a small constant so that the slab density has considerable spread. Having a diffuse slab allows vectors with large coefficients to escape the pull of the spike. If we also set λ_0 to be small, then the posterior will be relatively flat. However, with a diffuse spike *and* slab density, many negligible γ_k 's will tend to be selected in our model. To eliminate these suboptimal non-sparse modes, we then gradually increase λ_0 along a ladder of L increasing values, $\{\lambda_0^1, \dots, \lambda_0^L\}$. For each λ_0^s in the ladder, we reinitialize $(\gamma, \theta, \sigma^2, \rho^2)$ using the MAP estimate $(\hat{\gamma}_{s-1}, \hat{\theta}_s, \hat{\sigma}_{s-1}^2, \hat{\rho}_{s-1})$ from the previous spike parameter λ_0^{s-1} as a “warm start.” As we increase λ_0 , the posterior becomes “spikier,” with the spikes absorbing more and more negligible parameter estimates. For large enough λ_0 , the algorithm will eventually stabilize so that further increases in λ_0 do not change the solution.

The complete algorithm for the NVC-SSL model is given in Algorithm 1. Let $\mathbf{t} = (t_{11}, \dots, t_{1n_1}, \dots, t_{n_1}, \dots, t_{nn_n})'$ be the vector of all observation times for all subjects. Once we have gotten the final estimate $\hat{\gamma}$, we can obtain the estimates for the smooth functionals as $\hat{\beta}_k(\mathbf{t}) = \sum_{l=1}^d \hat{\gamma}_{kl} B_{kl}(\mathbf{t})$, $k = 1, \dots, p$,, where $\hat{\beta}_k(\mathbf{t})$ is a $N \times 1$ vector of $\hat{\beta}_k$ evaluated at all N time points in \mathbf{t} . We reiterate that Step 3 of the algorithm is also computed in parallel for each $m_h \in \{m_1, \dots, m_q\}$ in order to accelerate computing time.

3.3 Selection of Degrees of Freedom

By utilizing dynamic posterior exploration, we do not need to tune the hyperparameter λ_0 . However, we still need to choose the degrees of freedom d (i.e. the number of basis functions to use). To do this, we use the Akaike information criterion with a correction for small sample sizes (AIC_c) [18]. This correction ensures that if the sample size is small, AIC_c will be reluctant to overfit. Let $\hat{S} \subset \{1, \dots, p\}$ denote the indices of the estimated nonzero subvectors of γ , with cardinality $|\hat{S}| = \hat{s}$. In this context, the AIC_c is defined as

$$AIC_c = \log \left(\frac{\|\mathbf{R}^{-1/2}(\hat{\rho})(\mathbf{Y} - \mathbf{U}\hat{\gamma})\|_2^2}{N} \right) + 1 + \frac{2(\hat{s} + 1)}{N - \hat{s} - 2}, \quad (3.8)$$

where $(\hat{\gamma}, \hat{\rho})$ are the modal estimates under the NVC-SSL prior. Note that if (γ, ρ) were known, then the first term in (3.8) would be the maximum likelihood estimate (MLE) for $\log(\sigma^2)$. We select the d which minimizes AIC_c from a reasonable range of values.

Note that in our numerical studies, we also found that simply fixing d to be sufficiently large (e.g., $d = 8$) gave excellent performance under the

Algorithm 1 Nonparametric Varying Coefficient Spike-and-slab Lasso

Input: grid of increasing λ_0 values $I = \{\lambda_0^1, \dots, \lambda_0^L\}$ and initial values $\gamma^* = \gamma^{(0)}, \theta^* = \theta^{(0)}, \sigma^{2*} = \sigma^{2(0)}$

For $s = 1, \dots, L$:

1. Set iteration counter $t_s = 0$
2. Initialize $\gamma^* = \gamma^{(t_{s-1})}, \theta^* = \theta^{(t_{s-1})}, \sigma^{2*} = \sigma^{2(t_{s-1})}$
3. For each m_h in m_1, \dots, m_q :
 - (a) Set $\rho = m_h$ and set $\tilde{\mathbf{Y}} = \mathbf{R}^{-1/2}(m_h)\mathbf{Y}$ and $\tilde{\mathbf{U}} = \mathbf{R}^{-1/2}(m_h)\mathbf{U}$.
 - (b) While $\text{diff} > \varepsilon$
 - i. Increment t_s
 - E-step:**
 - ii. Compute $\lambda_k^* = \lambda_1 p_k^{*(t_{s-1})} + \lambda_0(1 - p_k^{*(t_{s-1})})$, $k = 1, \dots, p$, where $p_k^{*(t_{s-1})} = p^*(\gamma_k^{(t_{s-1})}, \theta^{(t_{s-1})})$ as in (3.3)
 - M-step:**
 - iii. Update $\theta^{(t_s)}$ given $\rho = m_h$ according to (3.5)
 - iv. Update $\gamma^{(t_s)}$ given $\rho = m_h$ by solving (3.6)
 - v. Update $\sigma^{2(t_s)}$ given $\rho = m_h$ according to (3.7)
 - vi. $\text{diff} = \|\gamma^{(t_s)} - \gamma^{(t_{s-1})}\|_2$
 - (c) Evaluate $\log \pi(\gamma^{(t_s)}, \theta^{(t_s)}, \sigma^{2(t_s)}, \rho | \mathbf{Y}, \rho = m_h)$ as in (3.1)
4. Set $\rho^{(t_s)}$ equal to the m_h that maximizes $\log \pi(\gamma^{(t_s)}, \theta^{(t_s)}, \sigma^{2(t_s)}, \rho | \mathbf{Y}, \rho = m_h)$, and set the corresponding $(\gamma^{(t_s)}, \theta^{(t_s)}, \sigma^{2(t_s)})$ given $\rho^{(t_s)}$ to be the final values for $(\gamma^{(t_s)}, \theta^{(t_s)}, \sigma^{2(t_s)})$

Return $\hat{\beta}_k(\mathbf{t}) = \sum_{l=1}^d \hat{\gamma}_{kl} B_{kl}(\mathbf{t})$, $k = 1, \dots, p$.

NVC-SSL model. Further tuning of d using AIC_c provided only modest improvements. This could possibly be attributed to the fact that the dynamic posterior exploration strategy from Section 3.2 already eliminates many spurious variables. In our simulations in Section 5, we use AIC_c to select d in order to make our comparisons with competing frequentist methods more transparent (where d was also similarly tuned). However, in practice, fitting the model with d large enough works quite well.

4 Asymptotic Theory for the NVC-SSL

In this section, we prove several asymptotic properties about the NVC-SSL model. To the very best of our knowledge, these are the first theoretical results for Bayesian NVC models when $p \gg n$. We assume that there is a

“true” model,

$$y_i(t_{ij}) = \sum_{k=1}^p x_{ik}(t_{ij})\beta_{0k}(t_{ij}) + \varepsilon_i(t_{ij}), i = 1, \dots, n, j = 1, \dots, n_i, \quad (4.1)$$

where $\varepsilon_i \sim \mathcal{N}_{n_i}(\mathbf{0}, \sigma_0^2 \mathbf{R}_i(\rho_0))$, $i = 1, \dots, n$ for fixed $\sigma_0^2 \in (0, \infty)$ and $\rho_0 \in (0, 1)$. We let \mathbb{P}_0 denote the probability measure underlying the true model (4.1). As before, suppose that each $\beta_{0k}(t)$ in (4.1) can be approximated by a linear combination of basis functions,

$$g_{0k}(t) = \sum_{i=1}^{d_k} \gamma_{0kl} B_{kl}(t), t \in T, k = 1, \dots, p, \quad (4.2)$$

where $\{B_{kl}, l = 1, \dots, d_k\}$ is a given basis system. Throughout this section, we assume that the basis functions are B-splines, as they are widely used in practice and the theory for B-splines is quite well-established. For simplicity, we also assume that $d_1 = \dots = d_p = d$, noting that this can be relaxed. Our theory will continue to hold if we allow different vector sizes d_k ’s, provided that we add the additional constraint that $\limsup_n d_{\max}/d_{\min} < \infty$, as in [16]. Our results would also then be expressed in terms of d_{\max} instead of d (see, e.g. Corollary 1 of [35]). For each $g_{0k}(t), k = 1, \dots, p$, let the approximation error be given by

$$\alpha_{0k}(t) = \beta_{0k}(t) - g_{0k}(t) = \beta_{0k}(t) - \sum_{l=1}^d \gamma_{0kl} B_{kl}(t), t \in T, k = 1, \dots, p,$$

and so model (4.1) can be written as

$$y_i(t_{ij}) = \sum_{k=1}^p \sum_{l=1}^d x_{ik}(t_{ij}) \gamma_{0kl} B_{kl}(t_{ij}) + \sum_{k=1}^p x_{ik}(t_{ij}) \alpha_{0k}(t_{ij}) + \varepsilon_i(t_{ij}). \quad (4.3)$$

Let $\boldsymbol{\delta}_0$ be an $N \times 1$ vector with entries, $\sum_{k=1}^p x_{ik}(\mathbf{t}) \alpha_{0k}(\mathbf{t})$. In matrix form, (4.1) can be expressed as

$$\mathbf{Y} = \mathbf{U} \boldsymbol{\gamma}_0 + \boldsymbol{\delta}_0 + \boldsymbol{\varepsilon}, \quad \boldsymbol{\varepsilon} \sim \mathcal{N}_N(\mathbf{0}, \sigma_0^2 \mathbf{R}(\rho_0)), \quad (4.4)$$

where \mathbf{U} is defined as in (2.5), $\boldsymbol{\gamma}_0 = (\gamma'_{01}, \dots, \gamma'_{0p})'$ where γ_{0k} is a d -dimensional vector of the true basis coefficients corresponding to the k th covariate, and $\mathbf{R}(\rho_0) = \text{diag}(\mathbf{R}_1(\rho_0), \dots, \mathbf{R}_n(\rho_0))$.

For our theoretical study of the NVC-SSL model, we endow $(\gamma_0, \sigma_0^2, \rho_0)$ in (4.4) with the prior,

$$\begin{aligned}\gamma &\sim \mathcal{SSGL}(\lambda_0, \lambda_1, \theta), \\ \sigma^2 &\sim \mathcal{IG}(c_0/2, d_0/2), \\ \rho &\sim \mathcal{U}(0, 1)\end{aligned}\tag{4.5}$$

where $c_0 > 0, d_0 > 0$, and $\theta \in (0, 1)$. Our theory builds upon recent work by [2] who studied posterior contraction rates for additive regression under the SSGL prior (2.8) and [19] who introduced a unified theoretical framework for sparse Bayesian regression models. Our work differs from [2] in that we no longer assume homoscedastic, uncorrelated errors, i.e. $\varepsilon \sim \mathcal{N}_N(\mathbf{0}, \sigma^2 \mathbf{I}_N)$. Our work also differs from [19] in that we use a *continuous* spike-and-slab prior that penalizes *groups* of coefficients, whereas [19] employ a point-mass spike-and-slab prior with a univariate Laplace density as the slab to penalize *individual* coefficients.

Remark 1. *For practical implementation of the NVC-SSL model, we endowed ρ with a discrete uniform prior. The prior we study here, i.e. $\rho \sim \mathcal{U}(0, 1)$, can be obtained as the limiting case when the number of atoms in (2.11) $q \rightarrow \infty$. Our theoretical results can also be shown to hold for the discrete uniform prior by making a few minor modifications to our proofs.*

4.1 Dimensionality Recovery for the NVC-SSL Model

We first begin with a result on dimensionality. Under our formulation (4.1), determining the number of nonzero functions $\beta_k(t)$ is equivalent to determining the number of d -dimensional vectors γ_k such that $\gamma_k \neq \mathbf{0}_d$. Since we used a continuous spike-and-slab prior in our prior formulation (4.5), our model assigns zero mass to exactly sparse vectors γ . To approximate the model size under the NVC-SSL model, we use the following generalized notion of sparsity [2]. For a small constant $\omega_d > 0$ which depends on d , we define the generalized inclusion indicator and generalized dimensionality, respectively, as

$$\nu_{\omega_d}(\gamma_k) = \mathbb{I}(\|\gamma_k\|_2 > \omega_d) \text{ and } |\nu(\gamma)| = \sum_{k=1}^p \nu_{\omega_d}(\gamma_k).\tag{4.6}$$

For the threshold ω_d , we use the following:

$$\omega_d \equiv \omega_d(\lambda_0, \lambda_1, \theta) = \frac{1}{\lambda_0 - \lambda_1} \log \left[\frac{1 - \theta}{\theta} \frac{\lambda_0^d}{\lambda_1^d} \right].\tag{4.7}$$

As noted in [2], any d -dimensional vectors γ_k satisfying $\|\gamma_k\|_2 = \omega_d$ represent the intersection points between the spike and the slab densities in the $\mathcal{SSL}(\lambda_0, \lambda_1, \theta)$ prior. For large λ_0 , the threshold ω_d rapidly approaches zero as n increases, so that $|\nu(\gamma)|$ provides a good approximation to $\#\{k : \gamma_k \neq \mathbf{0}_d\}$.

We first state the following regularity assumptions. We denote $\mathcal{H} := (0, \infty) \times (0, 1)$ as the parameter space for (σ^2, ρ) . Let $S_0 \subset \{1, \dots, p\}$ denote the set of indices of the true nonzero functions $\beta_{0k}(t)$ in (4.1), with cardinality $|S_0| = s_0$. Let $n_{\max} := \max\{n_1, \dots, n_n\}$ denote the maximum number of within-subject observations.

(A1) n, p, n_{\max} , and s_0 satisfy: $p \gg n, \log p = o(n), n_{\max} = O(1)$, and $s_0 = o(n/\log p)$.

(A2) The basis expansion dimension d satisfies:

$$1 \prec d \prec d \log d \prec n.$$

(A3) The eigenvalues of the within-subject correlation matrices satisfy

$$1 \lesssim \min_{1 \leq i \leq n} \lambda_{\min}(\mathbf{R}_i(\rho_0)) \leq \max_{1 \leq i \leq n} \lambda_{\max}(\mathbf{R}_i(\rho_0)) \lesssim 1.$$

(A4) For any $(\sigma_1^2, \rho_1), (\sigma_2^2, \rho_2) \in \mathcal{H}$,

$$\begin{aligned} \max_{1 \leq i \leq n} \|\sigma_1^2 \mathbf{R}_i(\rho_1) - \sigma_2^2 \mathbf{R}_i(\rho_2)\|_F^2 &\leq \frac{1}{n} \|\sigma_1^2 \mathbf{R}(\rho_1) - \sigma_2^2 \mathbf{R}(\rho_2)\|_F^2 \\ &\lesssim n_{\max}^2 (\sigma_1^2 - \sigma_2^2)^2 + n_{\max}^4 \sigma_2^4 |\rho_1 - \rho_2|^2. \end{aligned}$$

(A5) For \mathbf{U} in (4.4), define the matrix norm, $\|\mathbf{U}\|_* = \max_{1 \leq k \leq p} \|\mathbf{U}_k\|_2$, where \mathbf{U}_k is the submatrix of \mathbf{U} with d columns corresponding to the k th covariate. Suppose $\|\mathbf{U}\|_*^2 \asymp N$. Further, define the compatibility number $\phi_2(s)$ as

$$\phi_2(s) = \inf_{\gamma: 1 \leq |\nu(\gamma)| \leq s} \frac{\|\mathbf{U}\gamma\|_2}{\|\mathbf{U}\|_* \|\gamma\|_2},$$

and assume that for any constant $K > 0$, $\phi_2(Ks_0)$ is bounded away from zero.

(A6) $\|\gamma_0\|_\infty = O(\log p)$.

(A7) All the functions $\beta_k(t), k = 1, \dots, p$, are κ -times differentiable for $t \in T$ for some $\kappa > 0$.

- (A8) There exists a positive constant M such that $|x_{ik}(t_{ij})| \leq M$ for all $i = 1, \dots, n, j = 1, \dots, n_i, k = 1, \dots, p$.

Assumption (A1) allows the number of covariates p to grow at nearly exponential rate with sample size n . However, the true number of nonzero functions should grow slower than $n/\log p$. Assumption (A2) allows the dimension d to diverge as n grows, but places restrictions on its growth rate, à la [16]. Assumptions (A3)-(A4) ensure that the within-subject covariance matrices $\sigma^2 \mathbf{R}_i(\rho)$ are asymptotically well-behaved in some sense. In particular, Assumption (A3) states that the true within-subject correlation matrices should have bounded eigenvalues. Assumption (A4) ensures that for n subjects, the maximum squared Frobenius norm for the difference between two covariance matrices of dimension $n_i \times n_i, i = 1, \dots, n$, can be bounded above by a function of n_{\max} . In Theorem 9 of [19], it is shown that these two conditions hold for a wide class of covariance matrices, including compound symmetry, moving average (MA), and AR(1) covariance matrices (see Corollaries 1 and 2). Assumption (A5) controls the eigenstructure of the design matrix \mathbf{U} and is similar to restricted eigenvalue conditions or sparse Rietz conditions imposed elsewhere (see, e.g. [35, 2]). Assumption (A6) restricts the growth rate of the maximum signal size in γ_0 . Assumption (A7) defines the minimum smoothness for all additive functions, so that the bias incurred by a d -dimensional basis expansion is asymptotically on the order of $d^{-\kappa}$. Finally, Assumption (A8) assumes that all the covariates are uniformly bounded.

With all these ingredients, we state our first result. This next theorem establishes that the NVC-SSL posterior concentrates on sparse models of dimension no larger than a constant multiple of the true model size.

Theorem 1 (dimensionality). *Under model (4.4), suppose that we endow (γ, σ^2, ρ) with the prior (4.5). Suppose that Assumptions (A1)-(A8) hold. Further, assume that $\lambda_0 = (1 - \theta)/\theta = p^c$ where $c \geq 2$, and $\lambda_1 \asymp 1/n$. Then for sufficiently large $M_1 > 0$,*

$$\Pi(\gamma : |\nu(\gamma)| > M_1 s_0 | \mathbf{Y}) \rightarrow 0 \text{ a.s. } \mathbb{P}_0 \text{ as } n, p \rightarrow \infty.$$

Proof. Appendix B. □

Theorem 1 shows that the expected posterior probability that the generalized dimension size $|\nu(\gamma)|$ is a constant multiple larger than the true model size s_0 asymptotically vanishes. We also have the following corollary which shows that if the within-subject covariance matrices follow AR(1)

structure (for equally spaced time points) or compound symmetry, then the generalized dimensionality result of Theorem 1 holds.

Corollary 1. *Suppose the conditions for Theorem 1 hold. Let $\sigma_0^2 \in (0, \infty)$ and $\rho_0 \in (0, 1)$. If either: a) the within-subject matrices have AR(1) structure, i.e. the (j, k) th entry of \mathbf{R}_i is $\mathbf{R}_i(j, k) = \rho_0^{|j-k|}$, or b) the within-subject covariance matrices have compound symmetry structure, i.e. the (j, k) th entry of \mathbf{R}_i is $\mathbf{R}_i(j, k) = \mathbb{1}(j = k) + \rho_0(j \neq k)$, then for sufficiently large $M_1 > 0$,*

$$\Pi(\boldsymbol{\gamma} : |\boldsymbol{\nu}(\boldsymbol{\gamma})| > M_1 s_0 | \mathbf{Y}) \rightarrow 0 \text{ a.s. } \mathbb{P}_0 \text{ as } n, p \rightarrow \infty.$$

Proof. In the proof of Theorem 9 in [19], it is shown that under these conditions on the growth of n_{\max} , the within-subject covariance matrices $\sigma_0^2 R_i(\rho_0)$ satisfy both Assumptions (A3)-(A4). Thus, by Theorem 1, the dimensionality result holds. \square

4.2 Posterior Contraction Rate for the NVC-SSL Model

In addition to guaranteeing that the NVC-SSL posterior concentrates on sparse models, we also prove that our model consistently estimates the true functions $\boldsymbol{\beta}_0(\mathbf{t}) = (\beta_{01}(\mathbf{t}), \dots, \beta_{0p}(\mathbf{t}))'$ as $n, p \rightarrow \infty$. Let $\beta_k(\mathbf{t}) = \sum_{l=1}^{d_k} \gamma_{kl} B_{kl}(\mathbf{t})$ and $\beta_{0k}(\mathbf{t}) = \sum_{l=1}^{d_k} \gamma_{0kl} B_{kl}(\mathbf{t})$ denote $N \times 1$ vectors evaluated at the N observed time points, $\mathbf{t} = (t_{11}, \dots, t_{1n_1}, \dots, t_{n1}, \dots, t_{nn_n})'$. Let $\boldsymbol{\beta}(\mathbf{t}) = [\beta_1(\mathbf{t}), \dots, \beta_p(\mathbf{t})]$ and $\boldsymbol{\beta}_0(\mathbf{t}) = [\beta_{01}(\mathbf{t}), \dots, \beta_{0p}(\mathbf{t})]$ denote $N \times p$ matrices with respective columns $\beta_k(\mathbf{t})$ and $\beta_{0k}(\mathbf{t}), 1 \leq k \leq p$. We will position our results in terms of $\|\cdot\|_n$ neighborhoods of the truth, where

$$\|\boldsymbol{\beta}(\mathbf{t}) - \boldsymbol{\beta}_0(\mathbf{t})\|_n^2 = \frac{1}{n} \sum_{i=1}^n \frac{1}{n_i} \sum_{j=1}^{n_i} \sum_{k=1}^p [(\beta_k(t_{ij}) - \beta_{0k}(t_{ij}))^2].$$

The next theorem establishes nearly-optimal posterior concentration under the NVC-SSL prior, while the subsequent corollary shows that our posterior contraction result holds for NVC models with AR(1) and CS covariance structures.

Theorem 2 (posterior contraction rate). *Under model (4.4), suppose that we endow $(\boldsymbol{\gamma}, \sigma^2, \rho)$ with the prior (4.5). Suppose that Assumptions (A1)-(A8) hold. Further, assume that $\lambda_0 = (1 - \theta)/\theta = p^c$ where $c \geq 2$, and $\lambda_1 \asymp 1/n$. Then for $\epsilon_n = \sqrt{(s_0 \log p)/n} \vee d^{-\kappa}$,*

$$\Pi(\|\boldsymbol{\beta}(\mathbf{t}) - \boldsymbol{\beta}_0(\mathbf{t})\|_n > M_2 \epsilon_n | \mathbf{Y}) \rightarrow 0 \text{ a.s. } \mathbb{P}_0 \text{ as } n, p \rightarrow \infty,$$

for some $M_2 > 0$.

Proof. Appendix B. □

Corollary 2. *Suppose the conditions for Theorem 2 hold. Let $\sigma_0^2 \in (0, \infty)$ and $\rho_0 \in (0, 1)$. If either: a) the within-subject matrices have AR(1) structure, i.e. the (j, k) th entry of \mathbf{R}_i is $\mathbf{R}_i(j, k) = \rho_0^{|j-k|}$, or b) the within-subject covariance matrices have compound symmetry structure, i.e. the (j, k) th entry of \mathbf{R}_i is $\mathbf{R}_i(j, k) = \mathbb{1}(j = k) + \rho_0(j \neq k)$, then*

$$\Pi(\|\boldsymbol{\beta}(\mathbf{t}) - \boldsymbol{\beta}_0(\mathbf{t})\|_n > M_2 \epsilon_n | \mathbf{Y}) \rightarrow 0 \text{ a.s. } \mathbb{P}_0 \text{ as } n, p \rightarrow \infty,$$

for some $M_2 > 0$ and $\epsilon_n = \sqrt{(s_0 \log p)/n} \vee d^{-\kappa}$.

Theorem 2 and Corollary 2 show that the posterior contraction rate ϵ_n for the NVC-SSL model is the maximum of the error due to variable selection uncertainty (reflected in the term $\sqrt{(s_0 \log p)/n}$) and the approximation error from using basis expansions to estimate the smooth functionals (reflected in the term $d^{-\kappa}$). By Assumptions (A1)-(A2), both these terms tend towards zero as $n \rightarrow \infty$, indicating that the NVC-SSL model consistently estimates the true functionals $\boldsymbol{\beta}_0(t) = (\beta_{01}(t), \dots, \beta_{0p}(t))'$.

5 Simulations

For our simulation studies, we generate data from model (1.1) as follows. We have $n = 50$ subjects. To simulate the observation times, we first sample from $\{1, 2, \dots, 20\}$, where each time point has a 60 percent chance of being skipped. This way, we have irregularly spaced data, with n_i being different for different subjects. We then add random perturbation from $\mathcal{U}(-0.5, 0.5)$ to the non-skipped time points.

To ensure that we are in the high-dimensional scenario, we set $p = 400$, with the first six variables x_{i1}, \dots, x_{i6} being the relevant ones. $x_{i1}(t)$ is simulated from $\mathcal{U}(t/10, 2 + t/10)$ for any given time point t ; $x_{ij}(t), j = 2, \dots, 5$, conditioned on $x_{i1}(t)$, are iid drawn from a normal distribution with mean zero and variance $(1 + x_{i1}(t))/(2 + x_{i1}(t))$; x_{i6} , independent of $x_{ij}, j = 1, \dots, 5$ is normal with mean $3 \exp(t/30)$ and variance 1. For $k = 7, \dots, 400$, each $x_{ik}(t)$, independent of the others, is drawn from a multivariate normal distribution with covariance structure $\text{cov}(x_{ik}(t), x_{ik}(s)) = 2\rho^{-|t-s|}$, with $\rho = 0.8$. The coefficient functions are

$$\beta_1(t) = 20 \sin\left(\frac{\pi t}{15}\right), \beta_2(t) = 10 \cos\left(\frac{\pi t}{15}\right), \beta_3(t) = -1 + 2 \sin\left(\frac{\pi(t-25)}{15}\right),$$

$$\beta_4(t) = 2 - 2 \cos\left(\frac{\pi(t-25)}{15}\right), \beta_5(t) = 6 - 0.2t^2, \beta_6(t) = -4 + \frac{(20-t)^3}{2000},$$

$$\beta_7(t) = \dots = \beta_{400}(t) = 0.$$

To generate the random error $\varepsilon_i \stackrel{ind}{\sim} \mathcal{N}_{n_i}(\mathbf{0}, \sigma^2 \mathbf{R}_i(\rho))$, $i = 1, \dots, n$, we consider two cases: i) AR(1) where $\sigma^2 = 2$ and $\rho = 0.8$ (so that the (j, k) th entry of $\mathbf{R}_i(\rho)$ is $0.8^{|t_{ij} - t_{ik}|}$), and ii) CS where $\sigma^2 = 1$ and $\rho = 0.7$ (so that the (j, k) th entry of $\mathbf{R}_i(\rho)$ is $\mathbb{1}(j = k) + 0.7\mathbb{1}(j \neq k)$).

We evaluate both estimation performance and variable selection performance. To evaluate estimation quality, we compute the rescaled mean squared error $100 \times \text{MSE}$, where $\text{MSE} = (1/Np) \sum_{k=1}^p \sum_{i=1}^n \sum_{j=1}^{n_i} (\hat{\beta}_k(t_{ij}) - \beta_{0k}(t_{ij}))^2$. To evaluate variable selection performance, we compute the F1 score, which is defined as:

$$\text{F1} = \frac{2 \times \text{precision} \times \text{recall}}{\text{precision} + \text{recall}},$$

where $\text{precision} = \text{TP}/(\text{TP} + \text{FP})$, $\text{recall} = \text{TP}/(\text{TP} + \text{FN})$, and TP , FP , and FN denote the number of true positives, false positives, and false negatives respectively. A higher F1 score indicates that the model does a better job including relevant functions $\beta_k(t)$, while excluding irrelevant ones. We repeat our experiments 100 times and report the average MSE and F1 score.

To implement the NVC-SSL model, we fix the slab parameter $\lambda_1 = 0.1$ in the $\mathcal{SSGL}(\lambda_0, \lambda_1, \theta)$ prior (2.8) and use the dynamic posterior exploration strategy described in Section 3.2 for the spike parameter λ_0 , with a ladder $I = \{5, 10, 15, 20, 25\}$. We set $a = 1, b = p$ in the prior (2.9) on θ so that θ is small with high probability, and we set $c_0 = 1, d_0 = 1$ in the prior (2.10) on σ^2 , so that this prior is relatively noninformative. The discrete uniform prior on ρ (2.11) has support $\{0.05, 0.10, \dots, 0.95\}$. Finally, the degrees of freedom d is chosen from the range $\{3, 4, \dots, 10\}$ to minimize the AIC_c criterion (3.8) described in Section 3.3.

With $p = 400$ and $3 \leq d \leq 10$, we are estimating a total of between 1200 and 4000 unknown basis coefficients. Thus, it would be quite time-consuming to implement this model using MCMC. However, with the EM algorithm we introduced in Section 3, we may obtain MAP estimates for $\hat{\gamma}$ (and thus estimates of $\hat{\beta}_k(t), k = 1, \dots, p$) in a fraction of the time it would take to perform MCMC.

We compared our method to the group lasso (gLASSO), group smoothly clipped absolute deviation (gSCAD), and group minimax concave penalty (gMCP) [38, 15]. For high-dimensional NVC models, these models solve the

Table 1: Simulation results averaged across 100 replications.

AR(1) error structure

Method	100 × MSE	F1 Score
NVC-SSL	0.674	0.994
NVC-gLASSO	6.00	0.955
NVC-gSCAD	4.20	0.943
NVC-gMCP	2.25	0.929

Compound symmetry error structure

Method	100 × MSE	F1 Score
NVC-SSL	0.645	0.912
NVC-gLASSO	5.97	0.957
NVC-gSCAD	4.15	0.943
NVC-gMCP	2.22	0.930

following optimization problem:

$$\hat{\gamma} = \arg \max_{\gamma} \frac{1}{2} \|\mathbf{Y} - \mathbf{U}\gamma\|_2^2 + \sum_{k=1}^p \text{pen}_\lambda(\gamma_k),$$

where \mathbf{U} is defined as in (2.5) and $\text{pen}_\lambda(\cdot)$ is a penalty function that depends on a tuning parameter λ . These methods have been considered by numerous authors, e.g., [33, 34, 35]. Unlike the NVC-SSL model, however, the penalty function $\text{pen}_\lambda(\cdot)$ is fully separable. Further, these penalized frequentist methods all ignore the within-subject temporal correlations. We choose (λ, d) to minimize the AIC_c criterion $AIC_c = \|\mathbf{Y} - \mathbf{U}\hat{\gamma}\|_2^2/N + 1 + 2(\hat{s} + 1)/(N - \hat{s} - 2)$, where \hat{s} is the estimated number of nonzero functions. These models were implemented using the R package `grpreg`.

Table 1 shows the MSE and F1 score averaged across 100 replications. For both the AR(1) or CS within-subject error structures, the NVC-SSL has much lower estimation error than the frequentist methods. This suggests two things: 1) that it is beneficial to use a *non*-separable and self-adaptive penalty (as the NVC-SSL does through the prior on the mixing proportion θ (2.9)), and 2) that estimation quality improves if we account for the within-subject correlations in our estimation procedure. In terms of F1 score, all the methods perform fairly well, with the NVC-SSL model having the highest F1

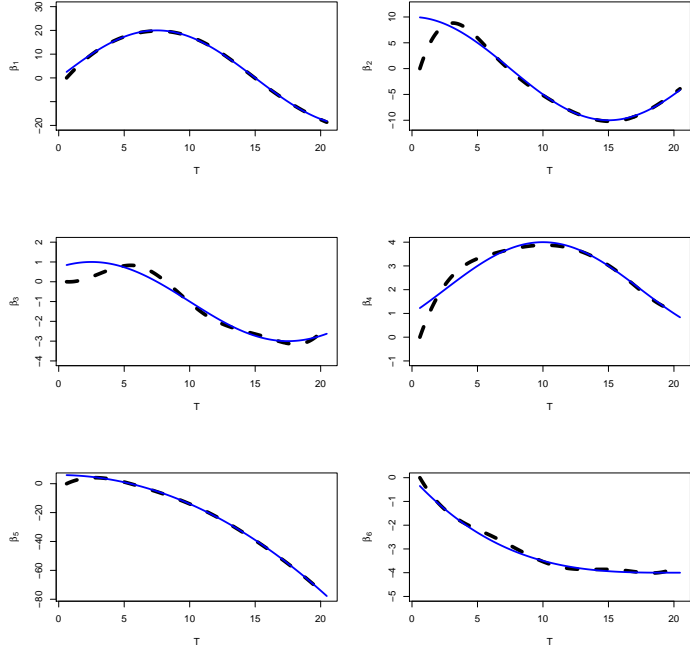


Figure 1: Plots of the estimates for $\beta_k(t)$, $k = 1, \dots, 6$, under the NVC-SSL model when the error terms follow AR(1) structure. The true functions are the solid lines and the NVC-SSL estimates are the dashed lines.

score for the AR(1) simulation. In the CS simulation, the gLasso approach has the highest F1 score but the estimation quality is the poorest.

In Figure 1, we plot the active functions $\beta_k(t)$, $k = 1, \dots, p$, against time t under the NVC-SSL for one replication of the AR(1) simulation. Figure 1 shows that the NVC-SSL is able to accurately estimate the unknown functions. Meanwhile, Figure 2 plots the functions estimated using the frequentist methods. For fairly large signals (β_1 , β_2 , and β_5), these methods performed fairly well. However, for the smaller signals (β_3 , β_4 , β_6), the estimation quality for the frequentist methods was not very good. This suggests that while ignoring temporal correlations may not have an adverse effect for large signals, it can be detrimental for estimation of smaller signals.

Our simulation results partly relied on the fact that we correctly specified the error covariance structure. In Appendix A, we illustrate through additional simulation studies that our model is also robust even when we have misspecified the error covariance. Even under misspecification, the NVC-

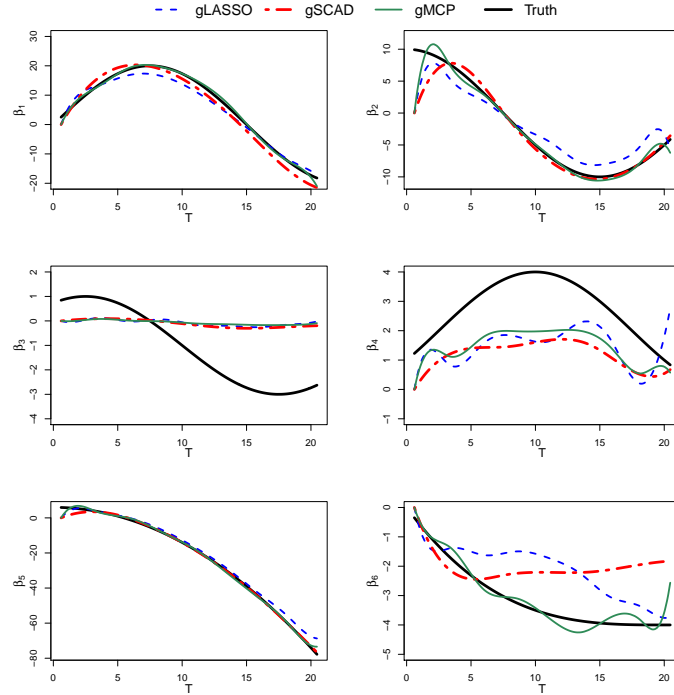


Figure 2: Plots of the estimates for $\beta_k(t)$, $k = 1, \dots, 6$, under the frequentist methods when the error terms follow AR(1) structure.

SSL model seems to outperform the frequentist methods which completely ignore the within-subject temporal correlations. Extending the NVC-SSL to specifically handle the issue of model robustness is a fruitful area for future research, and we outline a few thoughts on this in Section 7.

6 Analyzing Monthly Water Usage with the NVC-SSL Model

We illustrate the NVC-SSL method by modeling monthly water usage in Southwest Florida. This data set was first analyzed by Duerr et al. [6]. Monthly data was collected from 1998 to 2010 by Tampa Bay Water (TBW), a water authority operating within the Southwest Florida Water Management District (SWFWMD), for three member governments located in Hillsborough, Pasco, and Pinellas counties. This data set includes monthly water usage for each household based on billing records. This data set also con-

tains environmental covariates such as average monthly precipitation, average monthly evapotranspiration, and average monthly temperature, as well as household features like fraction of greenspace and land value.

For our analysis, we take monthly water usage as our time-varying response $y(t)$. Previous analysis in [6] suggested that monthly residential water usage follows a first-order autoregressive pattern. To apply the NVC-SSL method, we select a subset of 80 households from the year 2003. We then fit the NVC-SSL model with AR(1) errors to 41 continuous covariates, including the environmental covariates and household attributes listed above. Thus, our model is

$$y_i(t_{ij}) = \sum_{k=1}^{41} x_{ik}(t_{ij})\beta_k(t_{ij}) + \varepsilon_i(t_{ij}), i = 1, \dots, 80, j = 1, \dots, 12,$$

where $\varepsilon_i \sim \mathcal{N}_{12}(\mathbf{0}, \sigma^2 \mathbf{R}_i(\rho))$ and $\mathbf{R}_i(j, k) = \rho^{|j-k|}$. We use B-splines as the basis functions and select $d = 8$ as the degrees of freedom.

The NVC-SSL model selected 19 relevant predictors, including monthly average precipitation, average evapotranspiration, heated square footage, and fraction of greenspace. Figure 3 plots the estimated functions for four of the covariates determined to be significant by the NVC-SSL model.

7 Discussion

In this paper, we have introduced the nonparametric varying coefficient spike-and-slab lasso, a new Bayesian approach for estimation and variable selection in high-dimensional NVC models. The NVC-SSL model performs both estimation and variable of the functional components under model (1.1). Moreover, the NVC-SSL simultaneously estimates the covariance structure of the responses, whereas frequentist penalized approaches to NVC models tend to ignore these temporal correlations. Unlike frequentist approaches, the NVC-SSL model also employs a *non*-separable penalty which allows for automatic model complexity control and self-adaptivity to the true level of sparsity in the data. We introduced an efficient EM algorithm to obtain maximum *a posteriori* estimates, thus allowing us to bypass the use of MCMC. Finally, we provided theoretical support for the NVC-SSL by deriving the posterior contraction rates when $p \gg n$. To the best of our knowledge, there has not been any previous theoretical investigation of such high-dimensional Bayesian NVC models.

There are a few directions for future research. First, we could further relax some assumptions in our model. Although it is common practice to

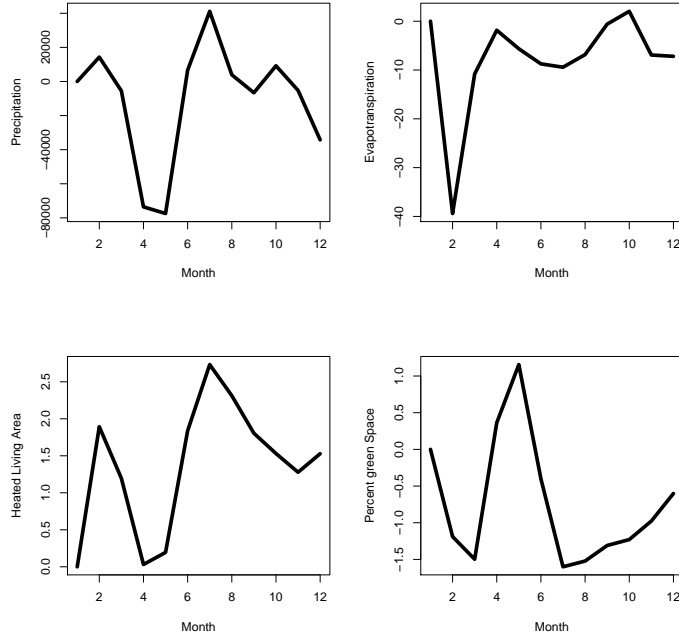


Figure 3: Plots of the functions for four of the relevant predictors: precipitation, evapotranspiration, heated living area, and fraction of greenspace.

model longitudinal data using either autoregressive or compound symmetry covariance structures for the random errors, these assumptions may be too simplistic. Additionally, it may be desirable to relax the assumption of Gaussian-distributed random errors. One possible way of addressing these issues is to model the ϵ_i 's nonparametrically using Dirichlet process mixture priors rather than multivariate Gaussians. We anticipate that the EM algorithm derived in this paper could be modified to accommodate such relaxations by using the stick-breaking representation of the Dirichlet process.

Another important issue is robustness of our procedure, particularly to misspecification of the temporal correlation structure. In the frequentist setting, a common approach for working around this issue is to use generalized estimating equations (GEEs), or pseudolikelihood methods [23, 39, 4, 10]. GEEs do *not* require the response to be normally distributed and only require the user to specify a “working” covariance structure. GEEs are known to consistently estimate the unknown parameters even if the covariance structure is misspecified [23, 4, 10]. It would be interesting to explore the

use of GEEs for Bayesian varying coefficient models. Under the Bayesian paradigm, replacing the likelihood with a pseudolikelihood would not yield a true posterior, but it is possible that the resultant “pseudo-posterior” would achieve both excellent finite-sample performance and posterior contraction at the (near) optimal rate [1]. We leave these extensions for future work.

Acknowledgments

Dr. Ray Bai and Dr. Mary Boland were funded in part by generous funding from the Perelman School of Medicine, University of Pennsylvania. Dr. Ray Bai and Dr. Yong Chen were funded by NIH grants 1R01AI130460 and 1R01LM012607. The authors are grateful to Seonghyun Jeong for helpful discussions. The TBW data set analyzed in Section 6 is not publicly available, but code to implement the simulation studies in Section 5 is available upon request.

References

- [1] Atchadé, Y. A. (2017). On the contraction properties of some high-dimensional quasi-posterior distributions. *Ann. Statist.*, 45(5):2248–2273.
- [2] Bai, R., Moran, G. E., Antonelli, J. L., Chen, Y., and Boland, M. R. (2019). Spike-and-slab group lassos for grouped regression and sparse generalized additive models. *arXiv preprint arXiv:1903.01979*.
- [3] Biller, C. and Fahrmeir, L. (2001). Bayesian varying-coefficient models using adaptive regression splines. *Statistical Modelling*, 1(3):195–211.
- [4] Chen, Y., Ning, J., and Cai, C. (2015). Regression analysis of longitudinal data with irregular and informative observation times. *Biostatistics*, 16(4):727–739.
- [5] Colman, P. (2004). Analysis of longitudinal data (second edition) diggle p, heagarty p, liang k-y, zeger s (2002) isbn 0198524846; 396 pages; £40.00, \$85.00 oxford university press; <http://www.oup.co.uk/isbn/0-19-852484-6>. *Pharmaceutical Statistics*, 3(2):147–148.
- [6] Duerr, I., Merrill, H. R., Wang, C., Bai, R., Boyer, M., Dukes, M. D., and Bliznyuk, N. (2018). Forecasting urban household water demand with statistical and machine learning methods using large space-time data: A comparative study. *Environmental Modelling & Software*, 102:29 – 38.

- [7] Fan, J. and Li, R. (2001). Variable selection via nonconcave penalized likelihood and its oracle properties. *Journal of the American Statistical Association*, 96(456):1348–1360.
- [8] Fan, J. and Zhang, J.-T. (2000). Two-step estimation of functional linear models with applications to longitudinal data. *Journal of the Royal Statistical Society. Series B (Statistical Methodology)*, 62(2):303–322.
- [9] Fan, J. and Zhang, W. (2008). Statistical methods with varying coefficient models. *Statistics and Its Interface*, 1(1):179–195.
- [10] Fang, E. X., Ning, Y., and Li, R. (2019). Test of significance for high-dimensional longitudinal data. *The Annals of Statistics (under revision)*.
- [11] Ghosal, S. and van der Vaart, A. (2017). *Fundamentals of Nonparametric Bayesian Inference*. Cambridge Series in Statistical and Probabilistic Mathematics. Cambridge University Press.
- [12] Hastie, T. and Tibshirani, R. (1993). Varying-coefficient models. *Journal of the Royal Statistical Society: Series B (Statistical Methodology)*, 55(4):757–796.
- [13] Hastie, T., Tibshirani, R., and Wainwright, M. (2015). *Statistical Learning with Sparsity: The Lasso and Generalizations*. Chapman & Hall/CRC.
- [14] Hoover, D. R., Rice, J. A., Wu, C. O., and Yang, L.-P. (1998). Nonparametric smoothing estimates of time-varying coefficient models with longitudinal data. *Biometrika*, 85(4):809–822.
- [15] Huang, J., Breheny, P., and Ma, S. (2012). A selective review of group selection in high-dimensional models. *Statist. Sci.*, 27(4):481–499.
- [16] Huang, J. Z., Wu, C. O., and Zhou, L. (2004). Polynomial spline estimation and inference for varying coefficient models with longitudinal data. *Statistica Sinica*, 14:763–788.
- [17] Huang, Z., Li, J., Nott, D., Feng, L., Ng, T.-P., and Wong, T.-Y. (2015). Bayesian estimation of varying-coefficient models with missing data, with application to the singapore longitudinal aging study. *Journal of Statistical Computation and Simulation*, 85(12):2364–2377.
- [18] Hurvich, C. M., Simonoff, J. S., and Tsai, C.-L. (1998). Smoothing parameter selection in nonparametric regression using an improved akaike

- information criterion. *Journal of the Royal Statistical Society. Series B (Statistical Methodology)*, 60(2):271–293.
- [19] Jeong, S. and Ghosal, S. (2019). A unified treatment of posterior asymptotics in sparse regression models. *pre-print*.
- [20] Krafty, R. T., Gimotty, P. A., Holtz, D., Coukos, G., and Guo, W. (2008). Varying coefficient model with unknown within-subject covariance for analysis of tumor growth curves. *Biometrics*, 64:1023–1031.
- [21] Kyung, M., Gill, J., Ghosh, M., and Casella, G. (2010). Penalized regression, standard errors, and bayesian lassos. *Bayesian Analysis*, 5(2):369–411.
- [22] Li, J., Wang, Z., Li, R., and Wu, R. (2015). Bayesian group lasso for nonparametric varying-coefficient models with application to functional genome-wide association studies. *The Annals of Applied Statistics*, 9(2):640–664.
- [23] Liang, K.-Y. and Zeger, S. L. (1986). Longitudinal data analysis using generalized linear models. *Biometrika*, 73(1):13–22.
- [24] Liang, K. Y. and Zeger, S. L. (1993). Regression analysis for correlated data. *Annual Review of Public Health*, 14(1):43–68. PMID: 8323597.
- [25] Liu, S. H., Bobb, J. F., Henn, B. C., Gennings, C., Schnaas, L., Tellez-Rojo, M., Bellinger, D., Arora, M., Wright, R. O., and Coull, B. A. (2018). Bayesian varying coefficient kernel machine regression to assess neurodevelopmental trajectories associated with exposure to complex mixtures. *Statistics in Medicine*, 25(3):665–683.
- [26] Moran, G. E., Ročková, V., and George, E. I. (2018). Variance prior forms for high-dimensional bayesian variable selection. *Bayesian Analysis (to appear)*.
- [27] Ning, B., Jeong, S., and Ghosal, S. (2018). Bayesian linear regression for multivariate responses under group sparsity. *ArXiv pre-print arXiv: 1807.03439*.
- [28] Qu, A. and Li, R. (2006). Quadratic inference functions for varying-coefficient models with longitudinal data. *Biometrics*, 62:379–391.
- [29] Rice, J. A. (2004). Functional and longitudinal data analysis: Perspectives on smoothing. *Statistica Sinica*, 14(3):631–647.

- [30] Ročková, V. and George, E. I. (2014). Emvs: The em approach to bayesian variable selection. *Journal of the American Statistical Association*, 109(506):828–846.
- [31] Ročková, V. and George, E. I. (2018). The spike-and-slab lasso. *Journal of the American Statistical Association*, 113(521):431–444.
- [32] Scott, J. G. and Berger, J. O. (2010). Bayes and empirical-bayes multiplicity adjustment in the variable-selection problem. *The Annals of Statistics*, 38(5):2587–2619.
- [33] Wang, H. and Xia, Y. (2009). Shrinkage estimation of the varying coefficient model. *Journal of the American Statistical Association*, 104(486):747–757.
- [34] Wang, L., Li, H., and Huang, J. Z. (2008). Variable selection in nonparametric varying-coefficient models for analysis of repeated measurements. *Journal of the American Statistical Association*, 103(484):1556–1569.
- [35] Wei, F., Huang, J., and Li, H. (2011). Variable selection and estimation in high-dimensional varying-coefficient models. *Statistica Sinica*, 21:1515–1540.
- [36] Wu, C. O. and Chiang, C.-T. (2000). Kernel smoothing on varying coefficient models with longitudinal dependent variable. *Statistica Sinica*, 10(2):433–456.
- [37] Xu, X. and Ghosh, M. (2015). Bayesian variable selection and estimation for group lasso. *Bayesian Analysis*, 10(4):909–936.
- [38] Yuan, M. and Lin, Y. (2006). Model selection and estimation in regression with grouped variables. *Journal of the Royal Statistical Society: Series B (Statistical Methodology)*, 68(1):49–67.
- [39] Zeger, S. L. and Liang, K.-Y. (1986). Longitudinal data analysis for discrete and continuous outcomes. *Biometrics*, 42(1):121–130.

A Simulation Study Under Misspecification

In this section, we illustrate the robustness of the NVC-SSL model to misspecification of the error covariance structure. We use the same setup of

Table 2: Simulation results under misspecification of the error covariance structure, averaged across 100 replications.

Method	100 × MSE	F1 Score
NVC-SSL-AR(1)	0.764	0.993
NVC-SSL-CS	0.740	0.905
NVC-gLASSO	5.97	0.959
NVC-gSCAD	4.16	0.943
NVC-gMCP	2.23	0.930

$n = 50$ and $p = 400$ as in Section 5. We use the same data-generating mechanism for generating observation times $\mathbf{t} = (t_{11}, \dots, t_{1n_1}, \dots, t_{n1}, \dots, t_{nn_n})'$ and time-varying covariates $x_{i1}(t), \dots, x_{ip}(t)$ and the same smooth functionals $\beta_k(t), k = 1, \dots, p$, as those in Section 5. However, for this simulation study, we specify the error covariance structure as a *mixture* of a first-order autoregressive (AR(1)) covariance matrix and a compound symmetry (CS) covariance matrix, i.e. $\boldsymbol{\varepsilon}_i \sim \mathcal{N}_{n_i}(0, \tilde{\mathbf{R}}_i)$, $i = 1, \dots, n$, where

$$\tilde{\mathbf{R}}_i = 0.5\sigma_1^2 \mathbf{R}_{1i}(\rho_1) + 0.5\sigma_2^2 \mathbf{R}_{2i}(\rho_2), \quad (\text{A.1})$$

and $\mathbf{R}_{1i}(\rho_1)$ has AR(1) structure with $(\rho_1, \sigma_1^2) = (0.7, 1.5)$, while $\mathbf{R}_{2i}(\rho_2)$ has CS structure with $(\rho_2, \sigma_2^2) = (0.3, 2)$.

Under (A.1), neither the AR(1) or CS covariance structures is correctly specified. We fit the NVC-SSL model with prespecified AR(1) structure and the NVC-SSL model with prespecified CS structure to the data with random errors generated from (A.1). We denote our models as NVC-SSL-AR(1) and NVC-SSL-CS respectively. We also fit the NVC-gLASSO, NVC-gSCAD, and NVC-gMCP models to the data for comparison.

Table 2 reports the rescaled mean squared error (100 × MSE) and the F1 score for our results averaged across 100 replications. The NVC-SSL-CS model performed the best in terms of estimation, despite the fact that the error covariance was not correctly specified. However, its F1 score was the lowest. The NVC-SSL-AR(1) method also had lower MSE than all of the frequentist methods and an F1 score very close to one, demonstrating that our method was still able to correctly identify signals in the data and threshold out noise variables under misspecification. Our results suggest that the NVC-SSL model is fairly robust to misspecification of the error covariance structure.

We caution that while the NVC-SSL model proved to be fairly robust in our simulations, it may not be robust under other types of misspecified

covariance structures. To tackle this issue, we would have to modify the NVC-SSL model to *specifically* address the issue of model robustness. This is beyond the scope of this article, and we leave such investigations for future research.

B Proofs of Main Results

In this section, we use the following notation. For two densities f and g , let $K(f, g) = \int f \log(f/g)$ and $V(f, g) = \int f |\log(f/g) - K(f/g)|^2$ denote the Kullback-Leibler (KL) divergence and variation respectively. Denote the Rényi divergence (of order 1/2) as $\rho(f, g) = -\log \int f^{1/2} g^{1/2} d\nu$. Finally, define the ε -covering number for a set Ω with semimetric d as the minimum number of d -balls of radius ε needed to cover Ω and denote the ε -covering number as $N(\varepsilon, \Omega, d)$ and the metric entropy as $\log N(\varepsilon, \Omega, d)$.

B.1 Proofs for Theorem 1

We first prove a lemma and then proceed to the proof of Theorem 1.

Lemma 1. *Let $f \sim \mathcal{N}_N(\mathbf{U}\boldsymbol{\gamma}, \sigma^2 \mathbf{R}(\rho))$ and $f_0 \sim \mathcal{N}_N(\mathbf{U}\boldsymbol{\gamma}_0 + \boldsymbol{\delta}_0, \sigma_0^2 \mathbf{R}(\rho_0))$. Under model (4.4), suppose that we endow $(\boldsymbol{\gamma}, \sigma^2, \rho)$ with the prior (4.5). Further, assume that $\lambda_0 = (1 - \theta)/\theta = p^c$ where $c \geq 2$, and $\lambda_1 \asymp 1/n$. Suppose that Assumptions (A1)-(A8) hold. Then $\sup_{\boldsymbol{\gamma}_0, \sigma_0^2, \rho_0} \mathbb{P}_0(E_n^c) \rightarrow 0$, where the set $E_n \equiv \left\{ \int \int \int \frac{f(\mathbf{Y})}{f_0(\mathbf{Y})} d\Pi(\boldsymbol{\gamma}) d\Pi(\sigma^2) d\Pi(\rho) \geq e^{-C_1 n \epsilon_n^2} \right\}$ for some constant $C_1 > 0$ and $\epsilon_n = \sqrt{(s_0 \log p)/n} \vee d^{-\kappa}$.*

Proof of Lemma 1. By Lemma 8.10 of [11], this statement will be proven if we can show that

$$\Pi \left(K(f_0, f) \leq n\epsilon_n^2, V(f_0, f) \leq n\epsilon_n^2 \right) \gtrsim \exp(-C_1 n \epsilon_n^2). \quad (\text{B.1})$$

For $\mathbf{R}_i^* = (\sigma^2/\sigma_0^2) \mathbf{R}_{0i}^{-1/2} \mathbf{R}_i \mathbf{R}_{0i}^{-1/2}$, $i = 1, \dots, n$, denote the ordered eigenvalues of \mathbf{R}_i^* by λ_{ij} , $1 \leq j \leq n_i$ and let $\mathbf{R}^* = \text{diag}(\mathbf{R}_1^*, \dots, \mathbf{R}_n^*)$. Using Lemma 6 of [19] and noting that the n subjects are independent, we have that

$$\begin{aligned} K(f_0, f) &= \frac{1}{2} \left\{ \sum_{i=1}^n \sum_{j=1}^{n_i} (\lambda_{ij} - 1 - \log \lambda_{ij}) + \frac{\|\mathbf{R}^{-1/2}(\mathbf{U}(\boldsymbol{\gamma} - \boldsymbol{\gamma}_0) - \boldsymbol{\delta}_0)\|_2^2}{\sigma^2} \right\}, \\ V(f_0, f) &= \left[\sum_{i=1}^n \sum_{j=1}^{n_i} \frac{(1 - \lambda_{ij})^2}{2} \right] + \frac{\sigma_0^2}{(\sigma^2)^2} \|\mathbf{R}_0^{1/2} \mathbf{R}^{-1}(\mathbf{U}(\boldsymbol{\gamma} - \boldsymbol{\gamma}_0) - \boldsymbol{\delta}_0)\|_2^2. \end{aligned}$$

Define the sets,

$$\begin{aligned}\mathcal{A}_1 &= \left\{ (\sigma^2, \rho) : \sum_{i=1}^n \sum_{j=1}^{n_i} (\lambda_{ij} - 1 - \log \lambda_{ij}) \leq n\epsilon_n^2, \sum_{i=1}^n \sum_{j=1}^{n_i} (1 - \lambda_{ij})^2 \leq n\epsilon_n^2 \right\}, \\ \mathcal{A}_2 &= \left\{ (\gamma, \sigma^2, \rho) : \frac{\|\mathbf{R}^{-1/2}(\mathbf{U}(\gamma - \gamma_0) - \delta_0)\|_2^2}{\sigma^2} \leq n\epsilon_n^2, \right. \\ &\quad \left. \frac{\sigma_0^2}{(\sigma^2)^2} \|\mathbf{R}_0^{1/2} \mathbf{R}^{-1}(\mathbf{U}(\gamma - \gamma_0) - \delta_0)\|_2^2 \leq \frac{n\epsilon_n^2}{2} \right\}.\end{aligned}$$

Then $\Pi(K(f_0, f) \leq n\epsilon_n^2, V(f_0, f) \leq n\epsilon_n^2) = \Pi(\mathcal{A}_2|\mathcal{A}_1)\Pi(\mathcal{A}_1)$. We will consider $\Pi(\mathcal{A}_1)$ and $\Pi(\mathcal{A}_2|\mathcal{A}_1)$ separately. Arguing as in Lemma 1 of [19], we may expand $\log \lambda_{ij}$ in the powers of $(1 - \lambda_{ij})$ to get $\lambda_{ij} - 1 - \log \lambda_{ij} \sim (1 - \lambda_{ij})^2/2$. Using Lemma 6 of [19], we also have that $\sum_{i=1}^n \sum_{j=1}^{n_i} (1 - \lambda_{ij})^2 \lesssim \sum_{i=1}^n \|\sigma^2 \mathbf{R}_i(\rho) - \sigma_0^2 \mathbf{R}_0(\rho_0)\|_F^2 = \|\sigma^2 \mathbf{R}(\rho) - \sigma_0^2 \mathbf{R}_0(\rho_0)\|_F^2$. Altogether, we have as a lower bound for $\Pi(\mathcal{A}_1)$,

$$\begin{aligned}\Pi(\mathcal{A}_1) &\geq \Pi\left((\sigma^2, \rho) : \|\sigma^2 \mathbf{R}(\rho) - \sigma_0^2 \mathbf{R}_0(\rho_0)\|_F^2 \leq b_1^2 n \epsilon_n^2\right) \\ &\gtrsim \Pi\left((\sigma^2, \rho) : n_{\max}^2 (\sigma^2 - \sigma_0^2)^2 + n_{\max}^4 \sigma_0^4 |\rho - \rho_0|^2 \leq b_1^2 n^2 \epsilon_n^2\right) \\ &\geq \Pi\left(\sigma^2 : |\sigma^2 - \sigma_0^2| \leq \frac{b_1 n \epsilon_n}{\sqrt{2} n_{\max}}\right) \Pi\left(\rho : |\rho - \rho_0| \leq \frac{b_1 n \epsilon_n}{\sqrt{2} \sigma_0^2 n_{\max}^2}\right) \\ &\gtrsim \exp(-C_1 n \epsilon_n^2 / 2),\end{aligned}\tag{B.2}$$

for some constants $b_1 > 0$ and $C_1 > 0$. The second line of the display comes from Assumption (A4) and the final line comes from the fact that σ^2 and ρ follow inverse gamma and uniform priors respectively.

Next, we focus on bounding $\Pi(\mathcal{A}_2|\mathcal{A}_1)$ from below. Arguing as in Lemma 5.1 of [27], $\mathcal{A}_1 \supset \{\|\sigma^{-2} \mathbf{R}^{-1}(\rho) - \sigma_0^2 \mathbf{R}_0^{-1}(\rho_0)\|_F \leq \epsilon_n/b_2\}$ for some constant $b_2 > 0$ and sufficiently large n , which then implies that $\|\sigma^{-2} \mathbf{R}^{-1}(\rho)\|_2 \lesssim 1$ and $\|\mathbf{R}^*\|_2 \lesssim 1$ (by using suitably modified arguments from the proof of Lemma 5.1 in [27]). Thus, conditional on \mathcal{A}_1 , the left-hand sides for both inequalities in the set \mathcal{A}_2 may be bounded above by a constant multiple of $\|\mathbf{U}(\gamma - \gamma_0) - \delta_0\|_2^2$.

For some constants $b_3, b_4 > 0$, we thus have as a lower bound for $\Pi(\mathcal{A}_2|\mathcal{A}_1)$,

$$\Pi(\mathcal{A}_2|\mathcal{A}_1) \gtrsim \Pi\left(\gamma : \|\mathbf{U}(\gamma - \gamma_0) - \delta_0\|_2^2 \leq \frac{n\epsilon_n^2}{2b_3}\right)$$

$$\begin{aligned}
&\geq \Pi \left(\boldsymbol{\gamma} : \|\boldsymbol{U}(\boldsymbol{\gamma} - \boldsymbol{\gamma}_0)\|_2^2 + \|\boldsymbol{\delta}_0\|_2^2 \leq \frac{n\epsilon_n^2}{4b_3} \right) \\
&\geq \Pi \left(\boldsymbol{\gamma} : \|\boldsymbol{U}\|_*^2 \left(\sum_{k=1}^p \|\boldsymbol{\gamma}_k - \boldsymbol{\gamma}_{0k}\|_2 \right)^2 + Nd^{-2\kappa} \leq \frac{n\epsilon_n^2}{4b_3} \right) \\
&\asymp \Pi \left(\boldsymbol{\gamma} : \left(\sum_{k=1}^p \|\boldsymbol{\gamma}_k - \boldsymbol{\gamma}_{0k}\|_2 \right)^2 + \frac{d^{-2\kappa}}{4b_4^2} \leq \frac{\epsilon_n^2}{2b_4^2} \right) \\
&\geq \Pi \left(\boldsymbol{\gamma} : \sum_{k=1}^p \|\boldsymbol{\gamma}_k - \boldsymbol{\gamma}_{0k}\|_2 \leq \frac{\epsilon_n}{2b_4} \right) \\
&\geq \Pi_{S_0} \left(\boldsymbol{\gamma} : \sum_{k \in S_0} \|\boldsymbol{\gamma}_k - \boldsymbol{\gamma}_{0k}\|_2 \leq \frac{\epsilon_n}{4b_4} \right) \Pi_{S_0^c} \left(\boldsymbol{\gamma} : \sum_{k \in S_0^c} \|\boldsymbol{\gamma}_k - \boldsymbol{\gamma}_{0k}\|_2 \leq \frac{\epsilon_n}{4b_4} \right) \\
&\geq \prod_{k \in S_0} \Pi \left(\boldsymbol{\gamma} : \|\boldsymbol{\gamma}_k - \boldsymbol{\gamma}_{0k}\|_2 \leq \frac{\epsilon_n}{4b_4 s_0} \right) \prod_{k \in S_0^c} \Pi \left(\boldsymbol{\gamma} : \|\boldsymbol{\gamma}_k\|_2^2 \leq \frac{\epsilon_n^2}{16(p - s_0)^2} \right) \\
&\gtrsim \exp(-C_1 n \epsilon_n^2 / 2), \tag{B.3}
\end{aligned}$$

where the third line is obtained from Assumptions (A7) and (A8). Specifically, by the properties of B-splines and our assumption of the uniform boundedness of the covariates, the bias $\boldsymbol{\delta}_0$ satisfies $\|\boldsymbol{\delta}_0\|_2 \lesssim \sqrt{Nd}^{-\kappa}$. The fourth line is obtained from Assumption (A5), and the fifth line is obtained by noting that $N \leq n \times n_{\max} \asymp n$ by Assumption (A1). The final line of the display can be obtained by suitably modifying the arguments in part I of the proof of Theorem 6.1 in [2]. Combining (B.2)-(B.3), we have that

$$\Pi(\mathcal{A}_2 | \mathcal{A}_1) \gtrsim \exp(-C_1 n \epsilon_n^2 / 2) \exp(-C_1 n \epsilon_n / 2) = \exp(-C_1 n \epsilon_n^2),$$

and thus the Kullback-Leibler condition (B.1) holds. Therefore, invoking Lemma 8.10 of [11], $\mathbb{P}_0(E_n^c) \rightarrow 0$, where E_n was defined in the lemma. \square

Proof of Theorem 1. Let $E_n = \left\{ \int \int \int \frac{f(\mathbf{Y})}{f_0(\mathbf{Y})} d\Pi(\boldsymbol{\gamma}) d\Pi(\sigma^2) d\Pi(\rho) \geq e^{-C_1 n \epsilon_n^2} \right\}$. Define the set $\mathcal{B}_n = \{\boldsymbol{\gamma} : |\boldsymbol{\nu}(\boldsymbol{\gamma})| \leq C_2 s_0\}$, where $C_2 > C_1$. Then we have

$$\mathbb{E}_0 \Pi(\mathcal{B}^c | \mathbf{Y}) \leq \mathbb{E}_0 \Pi(\mathcal{B}^c | \mathbf{Y}) \mathbb{1}_{E_n} + \mathbb{P}_0(E_n^c). \tag{B.4}$$

By Lemma (1), $\mathbb{P}_0(E_n^c) \rightarrow 0$ as $n \rightarrow \infty$, so to prove that $\mathbb{E}_0 \Pi(\mathcal{B}^c | \mathbf{Y}) \rightarrow 0$, it suffices to show that $\mathbb{E}_0 \Pi(\mathcal{B}^c | \mathbf{Y}) \mathbb{1}_{E_n} \rightarrow 0$. Now,

$$\Pi(\mathcal{B}_n^c | \mathbf{Y}) = \frac{\int \int \int_{\mathcal{B}_n^c} \frac{f(\mathbf{Y})}{f_0(\mathbf{Y})} d\Pi(\boldsymbol{\gamma}) d\Pi(\sigma^2) d\Pi(\rho)}{\int \int \int \frac{f(\mathbf{Y})}{f_0(\mathbf{Y})} d\Pi(\boldsymbol{\gamma}) d\Pi(\sigma^2) d\Pi(\rho)}. \tag{B.5}$$

On the event E_n , the denominator in (B.5) is bounded below by $e^{-C_1 n \epsilon_n^2}$.

An upper bound for the expected value of the numerator is

$$\mathbb{E}_0 \left(\int \int \int_{\mathcal{B}_n^c} \frac{f(\mathbf{Y})}{f_0(\mathbf{Y})} d\Pi(\boldsymbol{\gamma}) d\Pi(\sigma^2) d\Pi(\rho) \right) \leq \int_{\mathcal{B}_n^c} d\Pi(\boldsymbol{\gamma}) = \Pi(|\boldsymbol{\nu}(\boldsymbol{\gamma})| > C_2 s_0). \quad (\text{B.6})$$

Using the same arguments as those in the proof of Theorem 6.1 of [2], we have

$$\Pi(\boldsymbol{\gamma} : |\boldsymbol{\nu}(\boldsymbol{\gamma})| > C_2 s_0) \prec e^{-C_2 n \epsilon_n^2}. \quad (\text{B.7})$$

Combining (B.6)-(B.7), we have that $\mathbb{E}_0 \Pi(\mathcal{B}^c | \mathbf{Y}) \mathbb{1}_{E_n} \prec e^{-(C_2 - C_1) n \epsilon_n^2} \rightarrow 0$, since $C_2 > C_1$. This completes the proof. \square

B.2 Proofs for Theorem 2

In this section, we follow a technique recently developed by [27, 19]. We first prove posterior contraction with respect to average Rényi divergence (of order 1/2) in Lemma 2. Then we use our result to derive a posterior contraction rate for $\boldsymbol{\gamma}$ under prediction loss in Lemma 3, which will imply the result in Theorem 2.

Lemma 2 (posterior contraction with respect to the average Rényi divergence). *Let $f \sim \mathcal{N}_N(\mathbf{U}\boldsymbol{\gamma}, \sigma^2 \mathbf{R}(\rho))$ and $f_0 \sim \mathcal{N}_N(\mathbf{U}\boldsymbol{\gamma}_0 + \boldsymbol{\delta}_0, \sigma_0^2 \mathbf{R}(\rho_0))$. Under model (4.4), suppose that we endow $(\boldsymbol{\gamma}, \sigma^2, \rho)$ with the prior (4.5). Further, assume that $\lambda_0 = (1 - \theta)/\theta = p^c$ where $c \geq 2$, and $\lambda_1 \asymp 1/n$. Suppose that Assumptions (A1)-(A8) hold. Then*

$$\sup_{\boldsymbol{\gamma}_0} \mathbb{E}_0 \Pi \left(\frac{1}{n} \rho(f, f_0) \geq M_3 \epsilon_n^2 | \mathbf{Y} \right) \rightarrow 0 \text{ as } n, p \rightarrow \infty,$$

for some $M_3 > 0$, where $\epsilon_n = \sqrt{(s_0 \log p)/n} \vee d^{-\kappa}$.

Proof of Lemma 2. Let $\mathcal{B}_n = \{|\boldsymbol{\nu}(\boldsymbol{\gamma})| > M_1 s_0\}$ For every $\epsilon > 0$, we have

$$\mathbb{E}_0 \Pi \left(\frac{1}{n} \rho(f, f_0) > \epsilon | \mathbf{Y} \right) \leq \mathbb{E}_0 \Pi \left(\boldsymbol{\gamma} \in \mathcal{B}_n : \frac{1}{n} \rho(f, f_0) > \epsilon | \mathbf{Y} \right) + \mathbb{E}_0 \Pi(\mathcal{B}_n^c | \mathbf{Y}). \quad (\text{B.8})$$

By Theorem 1, the second term in (B.8) goes to zero. Thus, to prove posterior contraction for $\frac{1}{n} \rho(f, f_0)$, it suffices to prove that the first term in (B.8) tends to zero as $n, p \rightarrow \infty$ for $\epsilon = M_3 \epsilon_n^2$.

To prove that $\mathbb{E}_0 \Pi(\boldsymbol{\gamma} \in \mathcal{B}_n : \frac{1}{n} \rho(f, f_0) > M_3 \epsilon_n^2 | \mathbf{Y}) \rightarrow 0$, we will first show the existence of a sieve \mathcal{F}_n such that

$$\Pi(\mathcal{B}_n \setminus \mathcal{F}_n) \leq \exp(-(1 + C_1)n\epsilon_n^2), \quad (\text{B.9})$$

where C_1 is the constant from Lemma 1. Then on \mathcal{B}_n , we will construct a test function φ_n such that

$$\begin{aligned} \mathbb{E}_{f_0} \varphi_n &\lesssim e^{-n\epsilon_n^2}, \\ \sup_{f \in \mathcal{F}_n : \rho(f_0, f) > M_3 n \epsilon_n^2} \mathbb{E}_f (1 - \varphi_n) &\lesssim e^{-n\epsilon_n^2/16}. \end{aligned} \quad (\text{B.10})$$

Finally, we will show that the metric entropy $\log N(\epsilon_n, \mathcal{B}_n \cap \mathcal{F}_n, \rho(\cdot))$ can be asymptotically bounded above by a constant of $n\epsilon_n^2$, which will complete the proof (see Lemma D.3 of [11] for more details).

Consider the sieve,

$$\begin{aligned} \mathcal{F}_n = \left\{ (\boldsymbol{\gamma}, \sigma^2, \rho) : \|\boldsymbol{\gamma} - \boldsymbol{\gamma}_0\|_\infty \leq \frac{np}{\lambda_1}, 0 < \sigma^2 \leq e^{C_2 n \epsilon_n^2}, \right. \\ \left. e^{-C_2 n \epsilon_n^2} \leq \rho \leq 1 - e^{-C_2 n \epsilon_n^2} \right\}, \end{aligned} \quad (\text{B.11})$$

for some $C_2 > 0$. Then

$$\begin{aligned} \Pi(\mathcal{B}_n \setminus \mathcal{F}_n) &\leq \sum_{S: s \leq M_1 s_0} \Pi(\|\boldsymbol{\gamma} - \boldsymbol{\gamma}_0\|_\infty > np/\lambda_1) + \Pi\left(\sigma^2 > e^{C_2 n \epsilon_n^2}\right) \\ &\quad + \Pi\left(\rho < e^{-C_2 n \epsilon_n^2}\right) + \Pi\left(\rho > 1 - e^{-C_2 n \epsilon_n^2}\right). \end{aligned} \quad (\text{B.12})$$

Since $\sigma^2 \sim \mathcal{IG}(c_0/2, d_0/2)$ and $\rho \sim \mathcal{U}(0, 1)$, it is easy to verify that the last three terms on the right-hand side of (B.12) are upper bounded by $e^{-C_3 n \epsilon_n^2}$ for some $C_3 > 0$. Thus, we just need to show that the probability of the first term on the right-hand side of (B.12) is upper bounded by $e^{-C_4 n \epsilon_n^2}$ for some $C_4 > 0$. For a given $\boldsymbol{\gamma} = (\boldsymbol{\gamma}'_1, \dots, \boldsymbol{\gamma}'_p)'$, the probability that the generalized dimensionality for $\boldsymbol{\gamma}$ is of size s is bounded above by

$$\binom{p}{s} \left[\int_{\|\boldsymbol{\gamma}_k\| > \omega_d} \Pi(\boldsymbol{\gamma}_k) d\boldsymbol{\gamma}_k \right]^s \left[\int_{\|\boldsymbol{\gamma}_k\| \leq \omega_d} \Pi(\boldsymbol{\gamma}_k) d\boldsymbol{\gamma}_k \right]^{p-s} < \binom{p}{s} (2\theta)^s, \quad (\text{B.13})$$

where we used the fact that for $\|\boldsymbol{\gamma}_k\|_2 > \omega_d$, $\Pi(\boldsymbol{\gamma}_k) < 2\theta C_k \lambda_1^d e^{-\lambda_1 \|\boldsymbol{\gamma}_k\|_2} := 2\theta \Psi(\boldsymbol{\gamma}_k | \lambda_1)$ (where C_k is the normalizing constant for the group lasso density) and we bounded $\Pr(\|\boldsymbol{\gamma}_k\|_2 \leq \omega_d)$ from above by one.

For a model $S \subset \{1, \dots, p\}$ of size s , define the density $\check{\Pi}(\boldsymbol{\gamma}_S) = \prod_{k=1}^s \Psi(\boldsymbol{\gamma}_k | \lambda_1)$ and note that $\check{\Pi}(\boldsymbol{\gamma}_S) \leq e^{\lambda_1 \|\boldsymbol{\gamma}_0\|_2^2} \check{\Pi}(\boldsymbol{\gamma}_S - \boldsymbol{\gamma}_{0S})$. Then we have

$$\Pi\left(\|\boldsymbol{\gamma} - \boldsymbol{\gamma}_0\|_\infty^2 > (np/\lambda_1)^2 | |S| = s\right) \leq \Pi\left(\|\boldsymbol{\gamma} - \boldsymbol{\gamma}_0\|_2^2 > (np/\lambda_1)^2 | |S| = s\right)$$

$$\begin{aligned}
&= \int_{\{\gamma_S: \|\gamma_S - \gamma_{0S}\|_2^2 > (np/\lambda_1)^2 - \|\gamma_{0S^c}\|_2^2\}} \Pi(\gamma_S) d\gamma_S \\
&< e^{\lambda_1 \|\gamma_0\|_2} \int_{\{\gamma_S: \|\gamma_S - \gamma_{0S}\|_2^2 > (np/\lambda_1)^2 - \|\gamma_0\|_2^2\}} \check{\Pi}(\gamma_S - \gamma_0) d\gamma_S \\
&\leq e^{\lambda_1 \|\gamma_0\|_2} (2C_k \lambda_1^d)^s e^{-\lambda_1 \sqrt{(np/\lambda_1)^2 - \|\gamma_0\|_2^2}} \\
&< e^{-\lambda_1(np/\lambda_1) + 2\lambda_1 \|\gamma_0\|_2} \\
&\prec e^{-np + 2n^{1/2}} \\
&\prec e^{-C_4 n \epsilon_n^2}, \tag{B.14}
\end{aligned}$$

for any $C_4 > 0$. Note that by Assumption (A6), $\|\gamma_0\|_2 \leq \sqrt{p} \|\gamma_0\|_\infty \lesssim \sqrt{p} \log p \prec \sqrt{pn}$ and $\lambda_1 \asymp 1/n$, and thus, $(np/\lambda_1)^2 - \|\gamma_0\|_2^2 \prec (np/\lambda_1)^2$. In the third line, we used the fact that for $\|\gamma_k\|_2 > \omega_d$, $\Pi(\gamma_k) < 2C_k \lambda_1^d e^{-\lambda_1 \|\gamma_k\|_2}$. In the fifth line, we used the fact that $2C_k \lambda_1^d < 1$ and $|\sqrt{x} - \sqrt{y}| \leq \sqrt{|x - y|}$ for $x, y > 0$, and in the sixth line, we used the fact that $\lambda_1 \|\gamma_0\|_2 = \lambda_1 \|\gamma_{0S_0}\|_2 \lesssim (\sqrt{ds_0} \log p)/n \leq d^{1/2} (s_0 \log p)/n = o(n^{1/2})$. From (B.13)-(B.14), we have

$$\begin{aligned}
\sum_{S: s \leq M_1 s_0} \Pi(\|\gamma - \gamma_0\|_\infty > np/\lambda_1) &< e^{-C_4 n \epsilon_n^2} \sum_{s=1}^{\lfloor M_1 s_0 \rfloor} \binom{p}{s} (2\theta)^s \\
&\leq e^{-C_4 n \epsilon_n^2} \sum_{s=1}^{\infty} \left(\frac{2\theta e p}{s} \right)^s \\
&\lesssim e^{-C_4 n \epsilon_n^2}, \tag{B.15}
\end{aligned}$$

where in the second line, we used the fact that $\binom{p}{s} \leq (ep/s)^s$. In the third line, we used the fact that $\theta < \theta/(1 - \theta) = 1/p^c$ for some $c \geq 2$, so the summands in the second line above converge to zero as $n \rightarrow \infty$, and thus, the infinite geometric series is bounded above by a constant. Thus, combining (B.15) with the upper bounds for the last three terms in (B.12), we may choose some $C_5 > C_1 + 1$, so that (B.9) holds. This proves (B.9).

We now show the existence of a test so that (B.10) also holds. As in [27, 19], we first consider the most powerful Neyman-Pearson test $\phi_n = \mathbb{1}\{f_1/f_0 \geq 1\}$. Following the arguments in [27, 19], if the average Rényi divergence between f_0 and f_1 is bigger than ϵ_n^2 , then

$$\begin{aligned}
\mathbb{E}_{f_0} \phi_n &\leq e^{-n \epsilon_n^2}, \\
\mathbb{E}_{f_1} (1 - \phi_n) &\leq e^{-n \epsilon_n^2}. \tag{B.16}
\end{aligned}$$

Taking the maximum of all such tests ϕ_n gives the first inequality in (B.10).

From the second inequality in (B.16), we apply the Cauchy-Schwartz inequality to get

$$\mathbb{E}_f(1 - \phi_n) \leq \{\mathbb{E}_{f_1}(1 - \phi_n)\}^{1/2} \left\{ \mathbb{E}_{f_1} \left(\frac{f}{f_1} \right)^2 \right\}^{1/2}. \quad (\text{B.17})$$

Next, we show that $\mathbb{E}_{f_1}(f/f_1)^2$ is bounded above for every density with parameters such that

$$\begin{aligned} \|\mathbf{U}(\boldsymbol{\gamma} - \boldsymbol{\gamma}_1)\|_2^2 &\leq \frac{n\epsilon_n^2}{16}, \\ \frac{1}{n}\|\sigma^2 \mathbf{R}(\rho) - \sigma_1^2 \mathbf{R}(\rho_1)\|_F^2 &\leq \frac{\epsilon_n^4}{4n_{\max}^2}, \end{aligned} \quad (\text{B.18})$$

Denote $\mathbf{R}_i^* = (\sigma_1^2/\sigma^2) \mathbf{R}_i^{-1/2}(\rho) \mathbf{R}_i(\rho_1) \mathbf{R}_i^{-1/2}(\rho)$. We have by Assumptions (A3)-(A4) that for any such densities satisfying (B.18),

$$\begin{aligned} \max_{1 \leq i \leq n} \|\mathbf{R}_i^* - \mathbf{I}_{n_i}\|_2 &\leq \max_{1 \leq i \leq n} \|\sigma^{-2} \mathbf{R}_i^{-1}(\rho)\|_2 \|\sigma^2 \mathbf{R}_i(\rho) - \sigma_1^2 \mathbf{R}_i(\rho_1)\|_2 \\ &\lesssim \frac{1}{\sqrt{n}} \|\sigma^2 \mathbf{R}(\rho) - \sigma_1^2 \mathbf{R}(\rho_1)\|_F \\ &\lesssim \frac{\epsilon_n^2}{2n_{\max}}. \end{aligned}$$

Further, $\max_{1 \leq i \leq n} \|\mathbf{R}_i^* - \mathbf{I}_{n_i}\|_2$ is bounded below by $\max_{1 \leq i \leq n} |\text{eig}_k(\mathbf{R}_i^*) - 1|$ for every $k \leq n_i$, where eig_k denotes the k th ordered eigenvalue of \mathbf{R}_i^* . Thus, we have

$$1 - \frac{\epsilon_n^2}{2n_{\max}} \leq \min_{1 \leq i \leq n} \lambda_{\min}(\mathbf{R}_i^*) \leq \min_{1 \leq i \leq n} \lambda_{\max}(\mathbf{R}_i^*) \leq 1 + \frac{\epsilon_n^2}{2n_{\max}}. \quad (\text{B.19})$$

Since $\epsilon_n^2/n_{\max} \rightarrow 0$, (B.19) implies that $2\mathbf{R}_i^* - \mathbf{I}_{n_i}$ is nonsingular for every $i \leq n$, and hence, for every $(\boldsymbol{\gamma}_1, \sigma_1^2, \rho_1)$ satisfying (B.18),

$$\begin{aligned} \mathbb{E}_{f_1}(f/f_1)^2 &= \prod_{i=1}^n \left\{ \det(\mathbf{R}_i^*)^{1/2} \det(2\mathbf{I}_{n_i} - \mathbf{R}_i^{*-1})^{-1/2} \right\} \\ &\quad \times \exp \left\{ \sum_{i=1}^n \|(2\mathbf{R}_i^* - \mathbf{I}_{n_i})^{-1/2} \sigma^{-1/2} [\mathbf{R}_i^{-1/2}(\rho)] (\mathbf{U}^i(\boldsymbol{\gamma} - \boldsymbol{\gamma}_1))\|_2^2 \right\}. \end{aligned} \quad (\text{B.20})$$

Arguing as in (S10) in the Supplementary material of [19], we have that

$$\prod_{i=1}^n \det(\mathbf{R}_i^*)^{1/2} \det(2\mathbf{I}_{n_i} - \mathbf{R}_i^{*-1})^{-1/2} \leq e^{3n\epsilon_n^2/4}. \quad (\text{B.21})$$

Further, for every $(\gamma_1, \sigma_1^2, \rho_1)$ satisfying (B.18), we have that the exponent term in (B.20) is bounded above by

$$\max_{1 \leq i \leq n} \|(2\mathbf{R}_i^* - \mathbf{I}_{n_i})^{-1}\|_2 \max_{1 \leq i \leq n} \|\sigma^{-2} \mathbf{R}_i^{-1}(\rho)\|_2 \|\mathbf{U}(\gamma - \gamma_1)\|_2^2 \leq \frac{n\epsilon_n^2}{8}, \quad (\text{B.22})$$

since $\max_{1 \leq i \leq n} \|(2\mathbf{R}_i^* - \mathbf{I}_{n_i})^{-1}\|_2 \leq 2$ for large n and our assumption that $\max_{1 \leq i \leq n} \|\sigma^{-2} \mathbf{R}_i^{-1}\|_2 \lesssim 1$. Combining (B.21)-(B.22), $\mathbb{E}_{f_1}(f/f_1)^2$ in (B.20) is bounded above by $e^{7n\epsilon_n^2/8}$ for every density f_1 with $(\gamma_1, \sigma_1^2, \rho_1)$ satisfying (B.18).

To get the second inequality in (B.10), we plug in the upper bound of $e^{7n\epsilon_n^2/8}$ for $\mathbb{E}_{f_1}(f/f_1)^2$ and the upper bound of $e^{-n\epsilon_n^2}$ for $\mathbb{E}_{f_1}(1 - \phi_n)$ (given in (B.16)) into the right-hand side of (B.17). Taking the maximum of all tests ϕ_n constructed above thus yields the second inequality in (B.10).

To complete the proof, we need to show that the metric entropy of the densities satisfying (B.18) can be asymptotically bounded above by a constant multiple of $n\epsilon_n^2$. Note that on \mathcal{B}_n , we have $\|\mathbf{U}(\gamma - \gamma_1)\|_2^2 \leq \|\mathbf{U}\|_*^2 (\sum_{k=1}^p \|\gamma_k - \gamma_{1k}\|_2)^2 \leq \|\mathbf{U}\|_*^2 (s_{\gamma - \gamma_1} \sqrt{d} \|\gamma - \gamma_1\|_\infty)^2 \leq 4NdM_1^2 s_0^2 \|\gamma - \gamma_1\|_\infty^2$. Additionally, by Assumption (A4), the left-hand side of the second inequality in (B.18) can be bounded from above by $n_{\max}^2 (\sigma^2 - \sigma_1^2)^2 + e^{2C_2 n \epsilon_n^2} n_{\max}^4 (\rho - \rho_1)^2$ on \mathcal{F}_n . Thus, for densities f_1 satisfying (B.18), the metric entropy can be bounded above by

$$\begin{aligned} & \log N \left(\frac{\sqrt{n}\epsilon_n}{8M_1 s_0 \sqrt{d} \sqrt{N}}, \left\{ \gamma : |\nu(\gamma)| \leq M_1 s_0, \|\gamma - \gamma_0\|_\infty \leq \frac{np}{\lambda_1} \right\}, \|\cdot\|_\infty \right) \\ & + \log N \left(\frac{\epsilon_n^2}{\sqrt{8} n_{\max}^2}, \left\{ \sigma^2 : 0 < \sigma^2 \leq e^{C_2 n \epsilon_n^2} \right\}, |\cdot| \right) \\ & + \log N \left(\frac{\epsilon_n^2}{\sqrt{8} n_{\max}^3 e^{C_2 n \epsilon_n^2}}, \left\{ \rho : 0 < \rho < 1 \right\}, |\cdot| \right). \end{aligned} \quad (\text{B.23})$$

One can easily verify that the last two terms in (B.23) are upper bounded by a constant multiple of $n\epsilon_n^2$. For the first term in (B.23), note that for any small $\delta > 0$,

$$\begin{aligned} & N \left(\delta, \left\{ \gamma : |\nu(\gamma)| \leq M_1 s_0, \|\gamma - \gamma_0\|_\infty \leq \frac{np}{\lambda_1} \right\}, \|\cdot\|_\infty \right) \\ & \leq \binom{p}{M_1 s_0} \left(\frac{3np}{\lambda_1} \right)^{M_1 s_0} \\ & \leq \left(\frac{3np^2}{\delta \lambda_1} \right)^{M_1 s_0}, \end{aligned}$$

where we used the fact that $\binom{p}{M_1 s_0} \leq p^{M_1 s_0}$. Using the fact that $\lambda_1 \asymp 1/n$, we therefore have for some $b_5 > 0$ that the first term in (B.23) can be upper bounded by

$$\begin{aligned} M_1 s_0 \log \left(\frac{24 M_1 \sqrt{d} \sqrt{N} s_0 n^{3/2} p^2}{b_5 \epsilon_n} \right) &\lesssim s_0 \log \left(\left(\frac{n^{1/2}}{(s_0 \log p)^{1/2}} \vee d^\kappa \right) s_0 n^3 p^2 \right) \\ &\lesssim s_0 (\log s_0 + \log n + \log p) \\ &\lesssim n \epsilon_n^2, \end{aligned} \quad (\text{B.24})$$

where we used the fact that $d = o(n)$ and $N \asymp n$ by Assumption (A1) and the fact that $\kappa \in \mathbb{N}$ by Assumption (A7). Therefore, from (B.23)-(B.24), the metric entropy for the densities satisfying (B.18) can be bounded above by a constant multiple of $n \epsilon_n^2$. Therefore, the first term on the right-hand side of (B.8) tends to zero as $n, p \rightarrow \infty$ and this completes the proof. \square

Lemma 3 (posterior contraction with respect to prediction loss). *Assume the same conditions as those in Lemma 2. Then*

$$\sup_{\gamma_0} \mathbb{E}_0 \Pi \left(\gamma : \|\mathbf{U}(\gamma - \gamma_0)\|_2 \geq M_4 \sqrt{N} \epsilon_n \right) \rightarrow 0 \text{ as } n, p \rightarrow \infty,$$

for some $M_4 > 0$ and $\epsilon_n = \sqrt{(s_0 \log p)/n} \vee d^{-\kappa}$.

Proof of Lemma 3. By Lemma 2, we have posterior contraction with respect to average Rényi divergence $n^{-1} \rho(f, f_0)$. Note that

$$\begin{aligned} \frac{1}{n} \rho(f, f_0) &= -\frac{1}{n} \left[\sum_{i=1}^n \log \left\{ \frac{[\det(\sigma^2 \mathbf{R}_i(\rho))]^{1/4} [\det(\sigma_0^2 \mathbf{R}_i(\rho_0))]^{1/4}}{\det((\sigma^2 \mathbf{R}_i(\rho) + \sigma_0^2 \mathbf{R}_i(\rho_0))/2)^{1/2}} \right\} \right] \\ &\quad + \frac{1}{4n} \|(\sigma^2 \mathbf{R}(\rho) + \sigma_0^2 \mathbf{R}(\rho_0))^{-1} (\mathbf{U}(\gamma - \gamma_0) - \boldsymbol{\delta}_0)\|_2^2. \end{aligned}$$

Then $n^{-1} \rho(f, f_0) \lesssim \epsilon_n^2$ implies that

$$\frac{1}{n} \sum_{i=1}^n \log \left\{ \frac{[\det(\sigma^2 \mathbf{R}_i(\rho))]^{1/4} [\det(\sigma_0^2 \mathbf{R}_i(\rho_0))]^{1/4}}{\det((\sigma^2 \mathbf{R}_i(\rho) + \sigma_0^2 \mathbf{R}_i(\rho_0))/2)^{1/2}} \right\} \lesssim \epsilon_n^2, \quad (\text{B.25})$$

and

$$\frac{1}{4n} \|(\sigma^2 \mathbf{R}(\rho) + \sigma_0^2 \mathbf{R}(\rho_0))^{-1} (\mathbf{U}(\gamma - \gamma_0) - \boldsymbol{\delta}_0)\|_2^2 \lesssim \epsilon_n^2. \quad (\text{B.26})$$

As in Theorem 3 of [19], define g as

$$g^2(\sigma^2 \mathbf{R}_i(\rho), \sigma_0^2 \mathbf{R}_i(\rho_0)) = 1 - \frac{[\det(\sigma^2 \mathbf{R}_i(\rho))]^{1/4} [\det(\sigma_0^2 \mathbf{R}_i(\rho_0))]^{1/4}}{\det((\sigma^2 \mathbf{R}_i(\rho) + \sigma_0^2 \mathbf{R}_i(\rho_0))/2)^{1/2}}.$$

Then using the inequality $\log x \leq x - 1$, (B.26) implies that

$$\epsilon_n^2 \gtrsim -\frac{1}{n} \sum_{i=1}^n \log[1 - g^2(\sigma^2 \mathbf{R}_i(\rho), \sigma_0^2 \mathbf{R}_i(\rho_0))] \geq \frac{1}{n} \sum_{i=1}^n g^2(\sigma^2 \mathbf{R}_i(\rho), \sigma_0^2 \mathbf{R}_i(\rho_0)).$$

By Lemma 6 of [19], $g^2(\sigma^2 \mathbf{R}_i(\rho), \sigma_0^2 \mathbf{R}_i(\rho_0)) \gtrsim \|\sigma^2 \mathbf{R}_i(\rho) - \sigma_0^2 \mathbf{R}_i(\rho_0)\|_F^2$ when $\epsilon_n^2 \rightarrow 0$, and therefore, we have that

$$\begin{aligned} \epsilon_n^2 &\gtrsim \frac{1}{n} \|\sigma^2 \mathbf{R}(\rho) - \sigma_0^2 \mathbf{R}(\rho_0)\|_F^2 \\ &\geq \max_{1 \leq i \leq n} \|\sigma^2 \mathbf{R}_i(\rho) - \sigma_0^2 \mathbf{R}_i(\rho_0)\|_2^2, \end{aligned}$$

where the second line of the display comes from Assumption (A4). By Assumption (A3) of the bounded eigenvalues of $\mathbf{R}(\rho_0)$, we also have

$$\begin{aligned} \max_{1 \leq i \leq n} \|\sigma^2 \mathbf{R}_i(\rho) + \sigma_0^2 \mathbf{R}_i(\rho_0)\|_2^2 \\ \leq 2 \max_{1 \leq i \leq n} \|\sigma^2 \mathbf{R}_i(\rho) - \sigma_0^2 \mathbf{R}_i(\rho_0)\|_2^2 + 8 \max_{1 \leq i \leq n} \|\sigma_0^2 \mathbf{R}_i(\rho_0)\|_2^2 \\ \lesssim \epsilon_n^2 + 1. \end{aligned} \tag{B.27}$$

Thus, combining (B.26)-(B.27), we have

$$\begin{aligned} \epsilon_n^2 &\geq \frac{1}{4n} \left(\max_{1 \leq i \leq n} \|\sigma^2 \mathbf{R}_i(\rho) + \sigma_0^2 \mathbf{R}_i(\rho)\|_2^{-2} \right) \|\mathbf{U}(\gamma - \gamma_0) - \delta_0\|_2^2 \\ &\gtrsim \frac{1}{n} \|\mathbf{U}(\gamma - \gamma_0) - \delta_0\|_2^2 / (1 + \epsilon_n^2), \end{aligned}$$

and thus $\rho(f, f_0) \lesssim n\epsilon_n^2$ implies that

$$\begin{aligned} \sqrt{n}\epsilon_n &\gtrsim \|\mathbf{U}(\gamma - \gamma_0) - \delta_0\|_2 / (1 + \epsilon_n^2)^{1/2} \\ &\geq (\|\mathbf{U}(\gamma - \gamma_0)\|_2 - \|\delta_0\|_2) / (1 + \epsilon_n^2)^{1/2} \\ &\gtrsim \|\mathbf{U}(\gamma - \gamma_0)\|_2 - M_5 \sqrt{N} d^{-\kappa} \\ &\gtrsim \|\mathbf{U}(\gamma - \gamma_0)\|_2 - M_5 \sqrt{N} \epsilon_n, \end{aligned} \tag{B.28}$$

for some $M_5 > 0$. In the third line of the above display, we used the fact that $\|\delta_0\|_2 \lesssim \sqrt{N} d^{-\kappa}$ by Assumptions (A7)-(A8). Thus, we have from (B.28) that the posterior is asymptotically supported on the event, $\{\gamma : \|\mathbf{U}(\gamma - \gamma_0)\|_2 \leq M_6 \sqrt{n}\epsilon_n + M_5 \sqrt{N} \epsilon_n\}$ for some $M_6 > 0$. However, $\sqrt{n}\epsilon_n \asymp \sqrt{N}\epsilon_n$, so the posterior is also asymptotically supported on the event $\{\|\mathbf{U}(\gamma - \gamma_0)\|_2 \leq M_4 \sqrt{N}\epsilon_n\}$ for some $M_4 > 0$. This completes the proof. \square

Proof of Theorem 2. First, we let $\mathbf{g}_0(\mathbf{t}) = [g_{01}(\mathbf{t}), \dots, g_{0p}(\mathbf{t})]$ and $\boldsymbol{\alpha}_0(\mathbf{t}) = [\alpha_{01}(\mathbf{t}), \dots, \alpha_{0p}(\mathbf{t})]$ be $N \times p$ matrices, where $\alpha_{0k}(\mathbf{t})$ is the approximation error for the k th basis expansion evaluated at \mathbf{t} , as in (4.3). We have

$$\begin{aligned}
\|\boldsymbol{\beta}(\mathbf{t}) - \boldsymbol{\beta}_0(\mathbf{t})\|_n^2 &= \|\boldsymbol{\beta}(\mathbf{t}) - \mathbf{g}_0(\mathbf{t}) + \mathbf{g}_0(\mathbf{t}) - \boldsymbol{\beta}_0(\mathbf{t})\|_n^2 \\
&\leq 2\|\boldsymbol{\beta}(\mathbf{t}) - \mathbf{g}_0(\mathbf{t})\|_n^2 + 2\|\boldsymbol{\alpha}_0(\mathbf{t})\|_n^2 \\
&\asymp \frac{\|\boldsymbol{\gamma} - \boldsymbol{\gamma}_0\|_2^2}{d} + \|\boldsymbol{\alpha}_0(\mathbf{t})\|_n^2 \\
&\lesssim d^{-1}\|\boldsymbol{\gamma} - \boldsymbol{\gamma}_0\|_2^2 + d^{-2\kappa} \\
&\lesssim \|\boldsymbol{\gamma} - \boldsymbol{\gamma}_0\|_2^2.
\end{aligned} \tag{B.29}$$

In the above display, we used assumptions (A3)-(A4) and Lemmas A.1 and A.2 of [16] in the third line. In the fourth line, we used Assumption (A7) – namely, by properties of B-splines, the approximation error satisfies $\|\sum_{k=1}^p \alpha_{0k}(\mathbf{t})\|_\infty = O(d^{-\kappa})$. Thus, we have $\|\boldsymbol{\alpha}_0(\mathbf{t})\|_n^2 \lesssim (1/n) \sum_{i=1}^n (1/n_i) \sum_{j=1}^{n_i} d^{-2\kappa} = d^{-2\kappa}$. In the final display, we used the fact that $d \succ 1$ by Assumption (A2). Following from (B.29), we have that for sufficiently large n ,

$$\{\|\boldsymbol{\beta}(\mathbf{t}) - \boldsymbol{\beta}_0(\mathbf{t})\|_n \geq M_2 \epsilon_n\} \subset \{\boldsymbol{\gamma} : \|\boldsymbol{\gamma} - \boldsymbol{\gamma}_0\|_2 \geq M_2 \epsilon_n\},$$

Therefore, in order to prove posterior contraction in the empirical norm for the smooth functionals, it suffices to prove that

$$\mathbb{E}_0 \Pi(\boldsymbol{\gamma} : \|\boldsymbol{\gamma} - \boldsymbol{\gamma}_0\|_2 \geq M_2 \epsilon_n | \mathbf{Y}) \rightarrow 0 \text{ as } n, p \rightarrow \infty. \tag{B.30}$$

By Theorem 1, the posterior is asymptotically supported on the event $\mathcal{B}_n = \{\boldsymbol{\gamma} : |\boldsymbol{\nu}(\boldsymbol{\gamma})| \leq M_1 s_0\}$. Thus, using the compatibility condition in Assumption (A5), we have $\|\mathbf{U}(\boldsymbol{\gamma} - \boldsymbol{\gamma}_0)\|_2 \geq \phi_2(M_1 s_0) \|\mathbf{U}\|_* \|\boldsymbol{\gamma} - \boldsymbol{\gamma}_0\|_2 \asymp \sqrt{N} \|\boldsymbol{\gamma} - \boldsymbol{\gamma}_0\|_2$. The result in Lemma 3 then immediately implies that (B.30) holds for $\boldsymbol{\gamma}$ under ℓ_2 error loss. Consequently, the smooth functionals also contract at the same rate ϵ_n with respect to the empirical norm. \square